Supplementary Information

π-Extended C_2-Symmetric Double NBN-Heterohelicenes with Exceptional Luminescent Properties

Zuobang Sun[†#], Chen Yi[‡#], Qifeng Liang[§], Chiranjeevi Bingi[†], Wenqing Zhu[‡], Peirong Qiang[†], Dongqing Wu[*†], Fan Zhang[*†]

[†]School of Chemistry and Chemical Engineering, State Key Laboratory of Metal Matrix Composites, Shanghai Jiao Tong University, Shanghai 200240, P. R. China

[‡]School of Materials Science and Engineering, Shanghai University, Shanghai 200072, P. R. China

[§]Department of Physics, Shaoxing University, 312000 Shaoxing, P. R. China

[#]These two authors contributed equally to this work

Table of Contents

1. Materials and Methods.

All the reagents were purchased from Sigma-Aldrich and Admas-beta, unless otherwise stated, the commercially available reagents and dry solvents were used without further purification. The reactions were performed using standard vacuum-line and Schlenk techniques, work-up and purification of all compounds were performed under air with reagent-grade solvents. Column chromatography was performed with silica gel (200-300 mesh). Analytical thin-layer chromatography (TLC) was performed on 0.2 mm silica gel coated glass sheets with F254 indicator. All yields given referred to isolated yields.

Nuclear magnetic resonance (NMR) spectra were measured on Mercury plus 400 or Bruker AVANCE III HD 500 spectrometers. ^{1}H NMR chemical shifts were referenced to tetramethylsilane (0 ppm), ^{13}C NMR chemical shifts were referenced to $CDCl_3$ (77.0 ppm). High-resolution electrospray ionization mass spectrometry was performed on a Ultra High Performance Liquid/Supercritical Fluid Chromatography - Quadrupole Time of Flight Mass Spectrometer (Waters: AcquityUPLC/UPC2/Xevo G2-XS QTOFMS) and MALDI-MS was performed on Fourier Transform Ion Cyclotron Resonance Mass Spectrometer (Bruker Daltonics: SolariX 7.0T FT ICR MS, Agilent 1260 HPLC). Ultraviolet-visible (UV-Vis) spectra were recorded on a Perkin Elmer Lambda 35 Spectrophotometer. The fluorescence spectroscopy (PL) emission spectra were obtained with a Perkin Elmer LS 55 spectrophotometer. The transient fluorescence decay characteristics and fluorescence quantum yields were measured using an Edinburgh Instrument FLS100 spectrometer. CD and CPL spectra were measured on Jasco J-810 spectropolarimeter and Jasco CPL 200, respectively. CV was performed in anhydrous DCM containing recrystallized tetra-n-butyl- ammoniumhexafluorophosphate ($TBAPF_6$, 0.1 M) as supporting electrolyte at 298 K. A conventional three electrode cell was used with a platinum working electrode (surface area of 0.3 mm^2) and a platinum wire as the counter electrode. The Pt working electrode was routinely polished with a polishing alumina suspension and rinsed with acetone before use. The measured potentials were recorded with respect to the Ag/AgCl reference electrode. All electrochemical measurements were carried out under an atmospheric pressure of nitrogen.

Synthetic Procedures

General Procedures: For reactions that require heating, the heat source is oil bath.

Scheme S1 Synthesis of **Br-NBN**

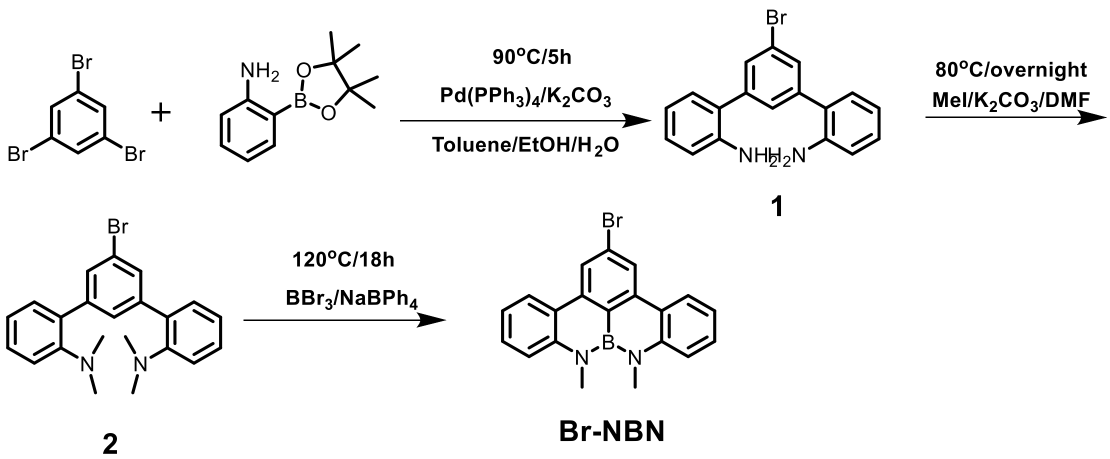

5'-bromo-[1,1':3',1''-terphenyl]-2,2''-diamine (1). In a 500 mL Schlenk flask, 1,3,5-tribromobenzene (5 g, 15.98 mmol), 2-(4,4,5,5-tetramethyl-1,3,2-dioxaborolan-2-yl)aniline(6.7 g, 31.8 mmol) and K_2CO_3 (13.2 g, 31.8 mmol) were charged under the protection of nitrogen. After adding 100 mL toluene, ethanol (28 mL) and H_2O (28 mL), the mixture was degassed for 30 min. $Pd(PPh_3)_4$ (923 mg, 0.8 mmol) was added, then the mixture was heated to 90 ^oC and stirred for 5 h. The resulting mixture was poured into brine and extracted with CH_2Cl_2 for three times. The combined organic layer was dried over anhydrous Na_2SO_4 and the solvents were removed under reduced pressure. The crude product was purified by silica gel column chromatography (petroleum ether : CH_2Cl_2 = 2:1) to give product as white powder (3.03 g, 56 %). ^1H NMR (400 MHz, $CDCl_3$) δ 7.61 (s, 2H), 7.52 (s, 1H), 7.19 – 7.12 (m, 4H), 6.84 – 6.76 (m, 4H), 3.79 (s, 4H). ^{13}C NMR (125 MHz, $CDCl_3$) δ 143.4, 142.0, 130.6, 130.4, 129.1, 128.5, 125.8, 123.2, 118.8, 115.8. HRMS *m/z* $[M+H]^+$ calculated for $C_{18}H_{16}BrN_2^+$ 341.0471 found 341.0482.

5'-bromo-N2,N2,N2'',N2''-tetramethyl-[1,1':3',1''-terphenyl]-2,2''-diamine (2). To a mixture of 5'-bromo-[1,1':3',1''-terphenyl]-2,2''-diamine (4.1 g, 12.2 mmol), K_2CO_3 (13.5 g, 97.4 mmol) and DMF (250 mL) was added MeI (17.3 g, 121.7 mmol). The mixture was heated to 80 ^oC and stirred overnight. The resulting mixture was poured into brine and extracted with CH_2Cl_2 for three times. The combined organic layer was dried over anhydrous Na_2SO_4 and the solvents were removed under reduced pressure. The crude product was purified by silica gel column chromatography (petroleum ether : CH_2Cl_2 = 4:1) to give product as white powder (4.73 g, 98 %). ^1H NMR (500 MHz, $CDCl_3$) δ 7.75 (s, 1H), 7.65 (d, *J* = 1.5 Hz, 2H), 7.30-7.28 (m, 2H), 7.23 (dd, *J* = 7.5, 1.5 Hz, 2H), 7.05(m, 4H), 2.59 (s, 12H). ^{13}C NMR (125 MHz, $CDCl_3$) δ 151.2, 143.9, 132.7, 131.5, 129.5, 128.5, 127.8, 122.1, 121.5, 117.7, 43.4. HRMS *m/z* $[M+H]^+$ calculated for $C_{22}H_{24}BrN_2^+$ 395.1117,397.1097; flound 395.1114, 397.1099.

2-bromo-8,9-dimethyl-8H,9H-8,9-diaza-8a-borabenzo[*fg*]tetracene (Br-NBN). In a 250 mL Schlenk tube, 5'-bromo-N2,N2,N2'',N2''-tetramethyl-[1,1':3',1''-terphenyl]-2,2''-diamine (4.6 g, 11.6 mmol) and $NaBPh_4$ (4.6 g, 17.3 mmol)were charged under the protection of nitrogen. After adding *o*-dichlorobenzene (55 mL) and BBr_3 (13.9 mmol, 13.9 mL, 1M in CH_2Cl_2), the mixture was heated to 120 ^oC and stirred for 18 h. The resulting mixture was filtered, poured into brine and extracted with CH_2Cl_2 for three times. The combined organic layer was dried over anhydrous Na_2SO_4 and the solvents were removed under reduced pressure. The crude product was purified by silica gel column chromatography (petroleum ether : CH_2Cl_2 = 8:1) to give product as white powder (2.6 g, 60%). ^1H NMR (500 MHz, $CDCl_3$) δ 8.28 (s, 2H), 8.22 (dd, *J* = 8.0 Hz, 2H), 7.51-7.47 (m, 2H), 7.40 (d, *J* = 8.0 Hz, 2H), 7.19-7.16 (m, 2H), 3.61 (s, 6H). ^{13}C NMR (101 MHz, $CDCl_3$) δ 144.9, 139.8, 129.1, 125.9, 124.3, 122.6, 122.0, 120.1, 115.6, 37.5. ^{11}B NMR (128 MHz, $CDCl_3$) δ 29.7. HRMS *m/z* $[M+H]^+$ calculated for $C_{20}H_{17}BrN_2$ is 375.0663, 377.0642; found 375.0672, 377.0653.

Scheme S2 Synthesis of the boronic acid[S1]

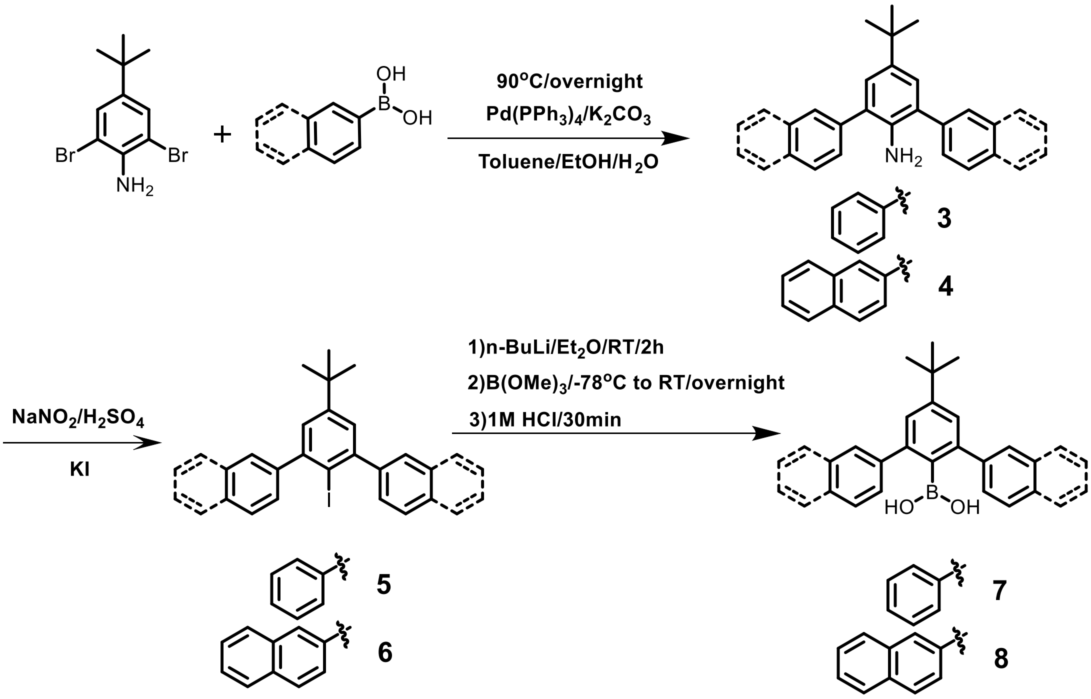

5'-(tert-butyl)-[1,1':3',1''-terphenyl]-2'-amine (3). In a 500 mL Schlenk flask, 2,6-dibromo-4-(tert-butyl)aniline (5.0 g, 16.2 mmol), phenylboronic acid (5.9 g, 48.8 mmol) and K_2CO_3 (22.5 g, 162.7 mmol)were charged under the protection of nitrogen. After adding toluene (150 mL), ethanol (35 mL) and H_2O (35 mL), the mixture was degassed for 30 min. $Pd(PPh_3)_4$ (0.95 g, 0.8 mmol) was added, then the mixture was heated to 90 ^oC and stirred overnight. The resulting mixture was poured into brine and extracted with CH_2Cl_2 for three times. The combined organic layer was dried over anhydrous Na_2SO_4 and the solvents were removed under reduced pressure. The crude product was purified by silica gel column chromatography (petroleum ether : CH_2Cl_2 = 4:1) to give product as white powder (4.5 g, 91 %). ^{1}H NMR ($CDCl_3$, 400 MHz): δ 7.55 (d, J = 7.2 Hz, 4H), 7.48 (t, J = 7.2 Hz, 4H), 7.37 (t, J = 7.2 Hz, 2H), 7.16 (s, 2H), 3.74 (s, 2H), 1.35 (s, 9H) ppm; ^{13}C NMR ($CDCl_3$, 125 MHz) 140.9, 140.2, 138.2, 129.4, 128.8, 127.6, 127.1, 126.8, 34.0, 31.6 ppm; HRMS (MALDI-FTICR): Calcd for $C_{22}H_{23}N$ 301.1830 found 301.1829

5'-(tert-butyl)-2'-iodo-1,1':3',1''-terphenyl (5). To a suspension of solid $NaNO_2$ (1.0 g, 13.9 mmol) conc. sulfuric acid (15 mL) was added a solution of 5'-(tert-butyl)-[1,1':3',1''-terphenyl]-2'-amine(4.0 g, 13.2 mmol) in acetic acid (20 mL) at 0 °C dropwise. After stirring for 1 h at 0 °C, the resulting mixture was added to a solution of KI (2.3 g, 13.9 mmol) in H_2O (35 mL) at 50 °C and stirred at 70 °C for 1 h. The reaction mixture were quenched with water and extracted with with CH_2Cl_2 for three times. The organic layer was washed with saturated hypo and dried over anhydrous Na_2SO_4 and the solvents were removed under reduced pressure. The crude product was purified by silica gel column chromatography (petroleum ether : CH_2Cl_2 = 10:1) to give product as white powder (3.8 g, 70 %).^{1}H NMR ($CDCl_3$, 500 MHz): δ 7.42-7.40 (m, 10H), 7.28 (s, 2H), 1.36 (s, 9H) ppm; ^{13}C NMR ($CDCl_3$, 125 MHz) 150.7, 147.5, 145.9, 129.5, 127.8, 127.4, 126.1, 99.8, 34.6, 31.2 ppm; HRMS(MALDI-FTICR): Calcd for $C_{22}H_{21}I$ 412.0688 found 412.0710

(5'-(tert-butyl)-[1,1':3',1''-terphenyl]-2'-yl)boronic acid (7). To a solution of 5'-(tert-butyl)-2'-iodo-1,1':3',1''-terphenyl (3.7 g, 8.9 mmol) in anhydrous diethyl ether (35 mL) was added *n*-BuLi (8.4 mL, 1.6 M, 13.4 mmol) dropwise via a syringe at room temperature under the protection of nitrogen. The mixture was stirred at room temperature for 2 h. After cooled to -78 ^{o}C, $B(OMe)_3$ (2.0 mL, 17.9 mmol) was added and the resulting mixture was stirred at RT overnight. The reaction mixture was quenched with HCl (1M), stirred for another 30 min and then extracted with CH_2Cl_2 for three times. The combined organic layer was dried over anhydrous Na_2SO_4 and the solvents were removed under reduced pressure. The crude product was purified by silica gel column chromatography (petroleum ether : CH_2Cl_2 = 1:2) to give product as white powder (1.8 g, 62%).^{1}H NMR ($CDCl_3$, 500 MHz) δ 7.49-7.48 (m, 4H), 7.45-7.36 (m, 8H), 4.09 (s, 2H), 1.38 (s, 9H) ppm; ^{13}C NMR ($CDCl_3$, 125 MHz) 152.2, 145.8, 143.6, 128.6, 128.5, 127.4, 125.3, 34.9, 31.3 ppm; HRMS (ESI-MS) $[M+Na]^+$: Calcd for $C_{22}H_{23}BNaO_2^+$ 353.1683 found 353.1683

4-(tert-butyl)-2,6-di(naphthalen-2-yl)aniline (4). In a 500 mL Schlenk flask, 2,6-dibromo-4-(tert-butyl)aniline (7.1 g, 23.2 mmol), naphthalen-2-ylboronic acid (9.9 g, 57.5 mmol) and K_2CO_3 (32.0 g, 232.5 mmol) were charged under the protection of nitrogen. After adding toluene (170 mL), ethanol (40 mL) and H_2O (40 mL), the mixture was degassed for 30 min. $Pd(PPh_3)_4$(1.3 g, 1.1 mmol) was added, then the mixture was heated to 90 ^{o}C and stirred overnight. The resulting mixture was poured into brine and extracted with CH_2Cl_2 for three times. The combined organic layer was dried over anhydrous Na_2SO_4 and the solvents were removed under reduced pressure. The crude product was purified by silica gel column chromatography (petroleum ether : CH_2Cl_2 = 4:1) to give product as white powder (8.1 g, 87 %). ^{1}H NMR ($CDCl_3$, 400 MHz): δ 8.02 (s, 2H), 7.95 (d, *J*=8.4 Hz, 2H), 7.89-7.88 (m, 4H), 7.71 (d, *J* = 8.4 Hz, 2H), 7.52-7.50 (m, 4H), 7.30 (s, 2H), 3.83 (s, 2H), 1.37 (s, 9H) ppm; ^{13}C NMR ($CDCl_3$, 125 MHz) 141.2, 138.6, 137.7, 133.6, 132.5, 128.4, 128.1, 128.0, 127.7, 127.7, 127.6, 127.1, 126.3, 126.0, 34.1, 31.6 ppm; HRMS(MALDI-FTICR): Calcd for $C_{30}H_{27}N$ 401.2143 found 401.2139

2,2'-(5-(tert-butyl)-2-iodo-1,3-phenylene)dinaphthalene (6). To a suspension of solid $NaNO_2$ (1.2 g, 18.2 mmol) conc. sulfuric acid (25 mL) was added a solution of 4-(tert-butyl)-2,6-di(naphthalen-2-yl)aniline (7.0 g, 17.4 mmol) in acetic acid (35 mL) at 0 °C dropwise. After stirring for 1 h at 0 °C, the resulting mixture was added to a solution of KI (3.0 g, 18.2 mmol) in H_2O (65 mL) at 50 °C and stirred at 70 °C for 1 h. The reaction mixture were quenched with water and extracted with with CH_2Cl_2 for three times. The organic layer was washed with saturated hypo and dried over anhydrous Na_2SO_4 and the solvents were removed under reduced pressure. The crude product was purified by silica gel column chromatography (petroleum ether : CH_2Cl_2 = 10:1) to give product as white powder (4.0 g, 45 %).^{1}H NMR ($CDCl_3$, 500 MHz): δ 7.91-7.88 (m, 6H), 7.85 (s, 2H), 7.58 (dd, *J* = 8.5, 1.5 Hz, 2H), 7.53-7.48 (m, 4H), 7.40 (s, 2H), 1.37 (s, 9H) ppm; ^{13}C NMR ($CDCl_3$, 125 MHz): δ 151.0, 147.5, 143.4, 133.0, 132.6, 128.1, 128.1, 128.0, 127.8, 127.2, 126.5, 126.2, 126.1, 99.8, 34.7, 31.3 ppm; HRMS(MALDI-FTICR): Calcd for $C_{30}H_{25}I$ 512.1001 found 512.1033

(4-(tert-butyl)-2,6-di(naphthalen-2-yl)phenyl)boronic acid (8). To a solution of 2,2'-(5-(tert-butyl)-2-iodo-1,3-phenylene)dinaphthalene (3.0 g, 5.9 mmol) in anhydrous diethyl ether (45 mL) was added *n*-BuLi (5.4 mL, 1.6 M, 8.74 mmol) dropwise via a syringe at room temperature under the protection of nitrogen. The mixture was stirred at room temperature for 2 h. After cooled to -78 °C, $B(OMe)_3$ (1.3 mL, 11.8 mmol) was added and the resulting mixture was stirred at RT overnight. The reaction mixture was quenched with HCl (1M), stirred for another 30 min and then extracted with CH_2Cl_2 for three times. The combined organic layer was dried over anhydrous Na_2SO_4 and the solvents were removed under reduced pressure. The crude product was purified by silica gel column chromatography (petroleum ether : CH_2Cl_2 = 1:2) to give product as white powder (1.0 g, 40 %). ^{1}H NMR ($CDCl_3$, 500 MHz): δ 7.96 (d, J = 1.0 Hz, 2H), 7.92-7.88(m, 6H), 7.66 (dd, J = 8.0, 1.5 Hz, 2H), 7.54 (s, 2H), 7.52-7.48 (m, 4H), 4.12 (s, 2H), 1.43 (s, 9H) ppm; ^{13}C NMR ($CDCl_3$, 125 MHz): δ 152.3, 145.9, 141.1, 133.4, 132.6, 128.2, 128.2, 127.8, 127.3, 127.1, 126.4, 126.1, 125.6, 35.0, 31.4 ppm; HRMS (ESI-MS) $[M+Na]^+$: Calcd for $C_{30}H_{27}BNaO_2$ 453.1996 found 453.1997

Scheme S3 Synthesis of **Ph-NBNDH** and **Naph-NBNDH**

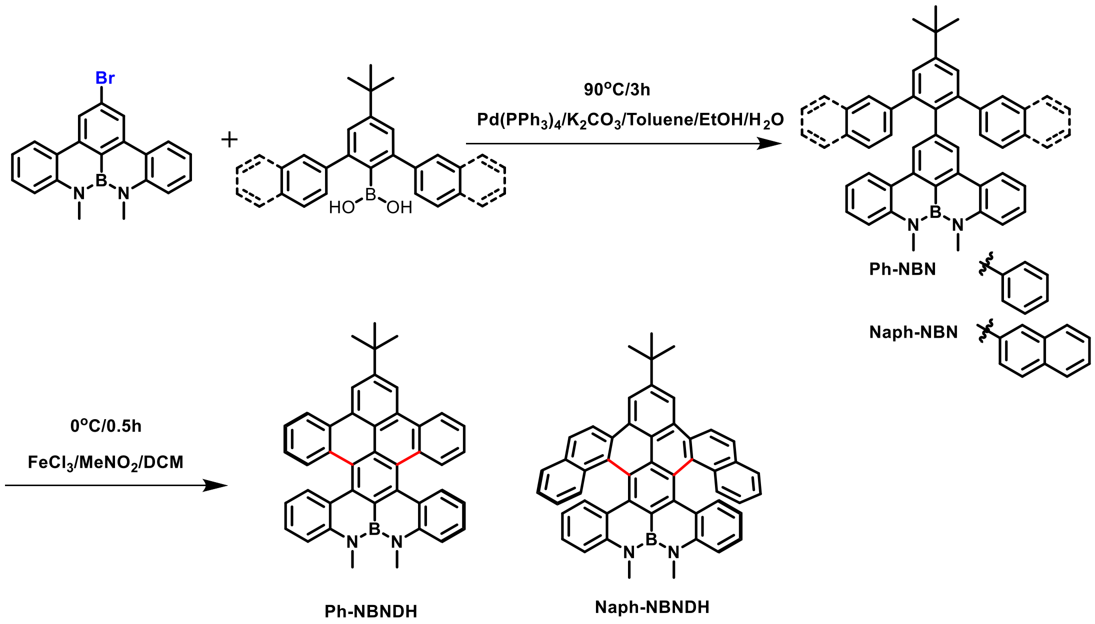

2-(5'-(tert-butyl)-[1,1':3',1''-terphenyl]-2'-yl)-8,9-dimethyl-8H,9H-8,9-diaza-8a-borabenzo[fg]tetracene (Ph-NBN). In a 100 mL Schlenk flask, 2-bromo-8,9-dimethyl-8H,9H-8,9-diaza-8a-borabenzo[fg]tetracene (375.0 mg, 1.0 mmol), (5'-(tert-butyl)-[1,1':3',1''-terphenyl]-2'-yl)boronic acid (396.0 mg, 1.2 mmol) and K_2CO_3 (1.38 g, 10 mmol) were charged under the protection of nitrogen. After adding toluene (25 mL), ethanol (7 mL) and H_2O (7 mL), the mixture was degassed for 30 min. $Pd(PPh_3)_4$ (115.0 mg, 0.1 mmol) was added, then the mixture was heated to 90 °C and stirred for 3 h. The resulting mixture was poured into brine and extracted with CH_2Cl_2 for three times. The combined organic layer was dried over anhydrous Na_2SO_4 and the solvents were removed under reduced pressure. The crude product was purified by silica gel column chromatography (petroleum ether : CH_2Cl_2 = 4 : 1) to give product as white powder (464.0 mg, 0.8 mmol, 80%). ^{1}H NMR (500 MHz, $CDCl_3$): δ 7.69 (s, 2H), 7.68 (dd, J=8.0, 1.5 Hz, 2H) , 7.55 (s, 2H), 7.38-7.35 (m, 2H), 7.31 (dd, J= 8.0, 0.5 Hz, 2H) , 7.20-7.18 (m, 4H), 7.11-7.07 (m, 4H), 7.03-6.98 (m, 4H), 3.54 (s, 6H), 1.47 (s, 9H); ^{13}C NMR (125 MHz, $CDCl_3$,): δ 150.3, 144.6, 142.5, 141.8, 141.1, 137.0, 136.5, 130.0, 128.0, 127.6, 126.9, 126.3, 124.1, 123.9, 123.5, 119.7, 115.2, 37.4, 34.8, 31.5; ^{11}B NMR (225 MHz, $CDCl_3$) δ 29.3; HRMS (MALDI-FTICR): Calcd for $C_{42}H_{37}BN_2$ 580.3050, found 580.3049

2-(4-(tert-butyl)-2,6-di(naphthalen-2-yl)phenyl)-8,9-dimethyl-8H,9H-8,9-diaza-8a-borabenzo [fg]tetracene (Naph-NBN). In a 100 mL Schlenk flask, 2-bromo-8,9-dimethyl-8H,9H-8,9-diaza-8a-borabenzo[fg]tetracene (375.0 mg, 1.0 mmol), (4-(tert-butyl)-2,6-di(naphthalen-2-yl)phenyl)boronic acid (516.0 ㎎, 1.2 mmol) and K_2CO_3 (1.4 g, 10.0 mmol) were charged under the protection of nitrogen. After adding toluene (25 mL), ethanol (7 mL) and H_2O (7 mL), the mixture was degassed for 30 min. $Pd(PPh_3)_4$ (115.0 mg, 0.1 mmol) was added, then the mixture was heated to 90 ^{o}C and stirred for 3 h. The resulting mixture was poured into brine and extracted with CH_2Cl_2 for three times. The combined organic layer was dried over anhydrous Na_2SO_4 and the solvents were removed under reduced pressure. The crude product was purified by silica gel column chromatography (petroleum ether : CH_2Cl_2 = 2 : 1) to give product as white powder (476.0 mg, 0.7 mmol, 70 %). ^{1}H NMR (400 MHz, $CDCl_3$): δ 7.89 (s, 2H), 7.82 (s, 2H) , 7.76 (d, *J*= 8.0 Hz, 2H), 7.66 (s, 2H), 7.60 (d, *J*= 8.0 Hz, 2H) , 7.54 (d, *J*=7.6 Hz, 2H), 7.44 (d, *J*=8.4 Hz, 2H), 7.39-7.35 (m, 2H), 7.32-7.28 (m, 4H), 7.23-7.21 (m, 2H), 7.18-7.16 (m, 2H), 6.83 (t, *J*= 6.8 Hz, 2H), 3.48 (s, 6H), 1.51 (s, 9H); ^{13}C NMR (125 MHz, $CDCl_3$,): δ 150.4, 144.5, 141.8, 141.0, 140.3, 136.6, 133.2, 131.9, 128.4, 128.4, 127.9, 127.8, 127.5, 127.4, 126.9, 125.7, 125.5, 124.0, 123.9, 123.9, 123.4, 119.6, 115.1, 37.3, 34.9, 31.5; ^{11}B NMR (225 MHz, $CDCl_3$) δ 29.1; HRMS (MALDI-FTICR): Calcd for $C_{50}H_{41}BN_2$ 680.3363, found 680.3354

20-(tert-butyl)-9,10-dimethyl-9H,10H-9,10-diaza-9a-borapentabenzo[a,cd,f,j,o] perylene (Ph-NBNDH). In a overdried 100 mL Schlenk flask, 2-(5'-(tert-butyl)-[1,1':3',1''-terphenyl]-2'-yl)-8,9-dimethyl-8H,9H-8,9-diaza-8a-borabenzo[fg] tetracene (**Ph-NBN**) (0.070 g, 0.12 mmol) was charged under the protection of nitrogen. After adding anhydrous CH_2Cl_2 (150 mL), the mixture was degassed for 30 min. Then the reactants were cold to 0 ^{o}C and $FeCl_3$ (0.48 mg, 3.00 mmol) in 3 mL nitromethane was added dropwise. After stirring at 0 ^{o}C for another 0.5 h, the resulting mixture was quenched with methanol and ice and extracted with CH_2Cl_2 for three times. The combined organic layer was dried over anhydrous Na_2SO_4 and the solvents were removed under reduced pressure. The crude product was purified by silica gel column chromatography (petroleum ether : ethyl acetate = 40 : 1) to give product as green powder (0.058 g, 83 %). ^{1}H NMR (500 MHz, $CDCl_3$): δ 9.01 (s, 2H), 8.76 (d, *J*=8.0 Hz, 2H) , 8.53 (d, *J*=8.0 Hz, 2H), 8.03 (dd, *J*= 8.0, 1.0 Hz, 2H), 7.57-7.53 (m, 4H) , 7.41-7.37 (m, 4H), 7.24-7.23 (m, 2H), 6.87-6.84 (m, 2H), 3.89 (s, 6H), 1.72 (s, 9H); ^{13}C NMR (125 MHz, $CDCl_3$,): δ 149.1, 144.2, 132.0, 131.8, 130.8, 130.3, 130.0, 129.8, 128.0, 127.7, 126.7, 125.6, 125.5, 123.4, 122.8, 121.2, 119.4, 118.6, 115.8, 37.8, 35.6, 31.9; ^{11}B NMR (225 MHz, $CDCl_3$): δ 27.9; HRMS (MALDI-FTICR): Calcd for $C_{42}H_{33}BN_2$ 576.2737, found 576.2742

24-(tert-butyl)-11,12-dimethyl-11H,12H-11,12-diaza-11a-boratribenzo[cd,j,o] dinaphtho[1,2-a:2',1'-f]perylene (Naph-NBNDH). In a overdried 100 mL Schlenk flask, 2-(4-(tert-butyl)-2,6-di(naphthalen-2-yl)phenyl)-8,9-dimethyl-8H,9H-8,9-diaza-8a-borabenzo[fg]t etracene (**Naph-NBN**) (0.10 g, 0.15 mmol) was charged under the protection of nitrogen. After adding anhydrous CH_2Cl_2 (150 mL), the mixture was degassed for 30 min. Then the reactants were cold to 0 °C and $FeCl_3$ (0.71g, 4.40 mmol) in 3 mL nitromethane was added dropwise. After stirring at 0 °C for another 0.5 h, the resulting mixture was quenched with methanol and ice and extracted with CH_2Cl_2 for three times. The combined organic layer was dried over anhydrous Na_2SO_4 and the solvents were removed under reduced pressure. The crude product was purified by silica gel column chromatography (petroleum ether : ethyl acetate = 40 : 1) to give product as orange powder (0.049 g, 49 %). ^{1}H NMR (400 MHz, $CDCl_3$): δ 9.12 (s, 2H), 8.96 (d, *J*=8.8 Hz, 2H) , 8.08 (d, *J*=8.8 Hz, 2H), 8.00 (d, *J*= 8.4 Hz, 2H), 7.84 (d, *J*= 7.6 Hz, 2H) , 7.51 (d, *J*= 8.4 Hz, 2H), 7.24-7.22 (m, 2H), 7.14-7.07 (m, 4H), 6.86 (t, *J*= 7.2 Hz, 2H), 6.33 (t, *J*= 7.2 Hz, 2H), 4.01 (s, 6H), 1.76 (s, 9H); ^{13}C NMR (125 MHz, $CDCl_3$,): δ 149.1, 143.7, 143.6, 134.1, 132.5, 130.4, 129.8, 129.8, 128.7, 128.4, 127.7, 127.4, 127.2, 127.0, 125.8, 125.3, 124.6, 121.3, 120.9, 119.1, 118.7, 115.2, 38.1, 35.8, 32.0; ^{11}B NMR (225 MHz, $CDCl_3$): δ 28.3; HRMS (MALDI-FTICR): Calcd for $C_{50}H_{37}BN_2$ 676.3050, found 676.3074

2. Single-Crystal X-Ray Analysis[S2]

Ph-NBNDH: The single crystal was obtained by diffusing methanol vapor into its toluene solutions. Intensity data were collected at 173 K on a Bruker SMART CCD X-ray Diffractometer (APEX II) with Cu Kα radiation (λ = 1.54178 Å) and graphite monochrometer.

(a)

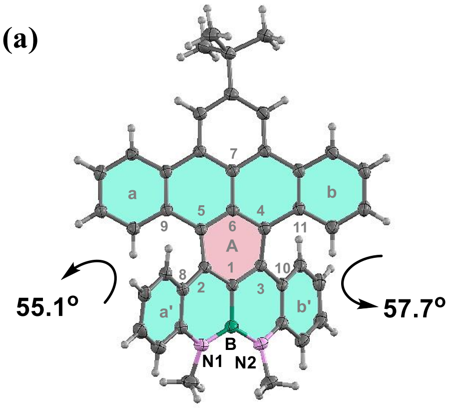

Top View

Selected bond length:

B-N1	**1.437(2) Å**
B-N2	**1.431(2) Å**
B-C1	**1.537(2) Å**
C1-C2	**1.404(2) Å**
C1-C3	**1.408(2) Å**
C2-C5	**1.421(2) Å**
C3-C4	**1.420(2) Å**
C2-C8	**1.471(2) Å**
C3-C10	**1.472(2) Å**
C5-C9	**1.468(2) Å**
C4-C11	**1.466(2) Å**
C6-C7	**1.451(2) Å**

Selected torsion angles:

C8-C2-C5-C9	**34.8°**
C10-C3-C4-C11	**34.4°**
C1-C2-C5-C6	**27.0°**
C1-C3-C4-C6	**26.8°**

Selected dihedral angles:

a-a' 55.1°
b-b' 57.7°

(b) **(c)**

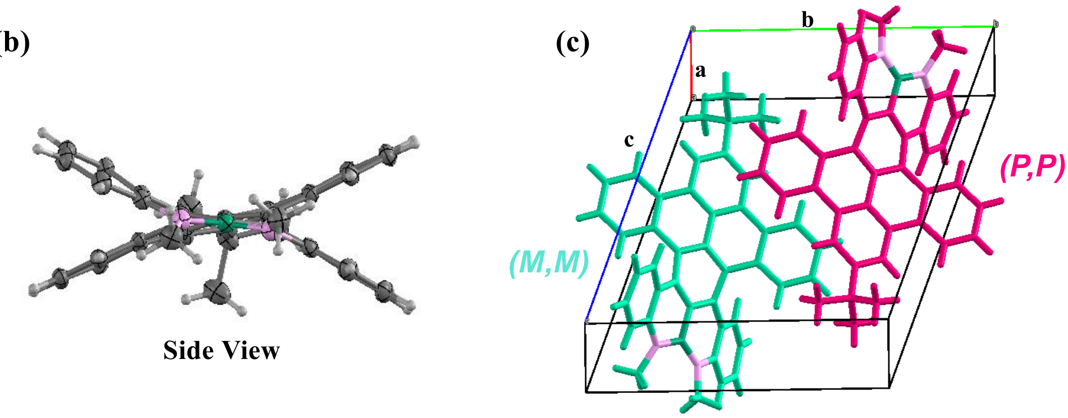

Side View

Figure S1 (a,b) X-ray crystal structures of **Ph-NBNDH** and selected crystal data. Thermal ellipsoids are shown at 50% probability. (c) Packing of one pair of enantiomers in one unit cell.

Table S1 Crystal data of **Ph-NBNDH** (CCDC: 1949280) :

Empirical formula	$C_{42} H_{33} B N_2$
Formula weight	576.51
Temperature/K	173(2)
Crystal system	triclinic
Space group	P-1
a/Å	7.22270(10)
b/Å	13.2949(2)
c/Å	15.8359(2)
α/°	100.1010(10)
β/°	99.8290(10)
γ/°	101.2940(10)
Volume/$Å^3$	1434.59(4)
Z	2
$\rho_{calc}g/cm^3$	1.335
μ/mm^{-1}	0.583
F(000)	608
Crystal size/mm^3	0.220 x 0.180 x 0.150
Radiation	CuKα (λ = 1.54178)
2Θ range for data collection/°	3.472 to 68.229
Index ranges	$-8 \leq h \leq 8, -15 \leq k \leq 16, -19 \leq l \leq 19$
Reflections collected	22409
Independent reflections	5240 [R(int) = 0.0311]
Data/restraints/parameters	5240 / 0 / 411
Goodness-of-fit on F^2	1.022
Final R indexes [I>=2σ (I)]	R1 = 0.0437, wR2 = 0.1198
R indices (all data)	R1 = 0.0512, wR2 = 0.1272
Largest diff. peak/hole / e $Å^{-3}$	0.241 and -0.182

Naph-NBNDH: The single crystal was obtained by diffusing methanol vapor into its toluene solutions. Intensity data were collected at 293 K on a Bruker SMART CCD X-ray Diffractometer (APEX II) with Cu Kα radiation (λ = 1.54178 Å) and graphite monochrometer.

(a)

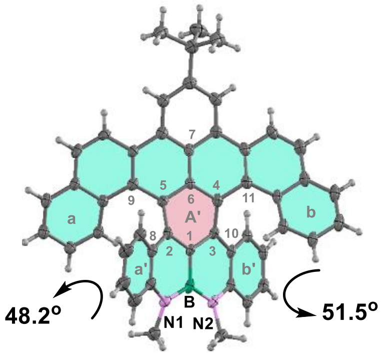

Top View

Selected bond length:

B-N1	**1.437(6) Å**
B-N2	**1.431(7) Å**
B-C1	**1.515(7) Å**
C1-C2	**1.410(7) Å**
C1-C3	**1.429(6) Å**
C2-C5	**1.403(7) Å**
C3-C4	**1.410(6) Å**
C2-C8	**1.466(7) Å**
C3-C10	**1.472(7) Å**
C5-C9	**1.469(7) Å**
C4-C11	**1.468(6) Å**
C6-C7	**1.407(6) Å**

Selected torsion angles:

C8-C2-C5-C9	**32.3°**
C10-C3-C4-C11	**29.5°**
C1-C2-C5-C6	**31.0°**
C1-C3-C4-C6	**29.6°**

Selected dihedral angles:

a-a'	**48.2°**
b-b'	**51.5°**

(b)

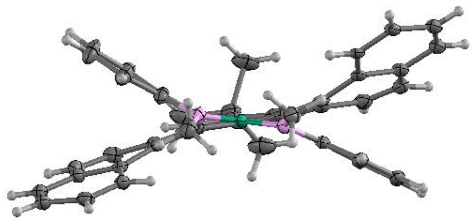

Side View

(c)

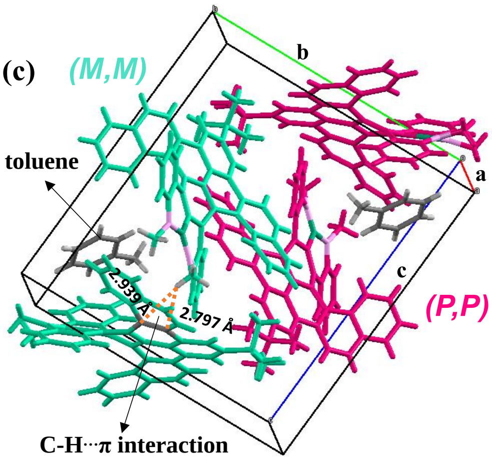

Figure S2 (a,b) X-ray crystal structures of **Naph-NBNDH** and selected crystal data. Thermal ellipsoids are shown at 30% probability. (c) Packing of two pairs of enantiomers in one unit cell.

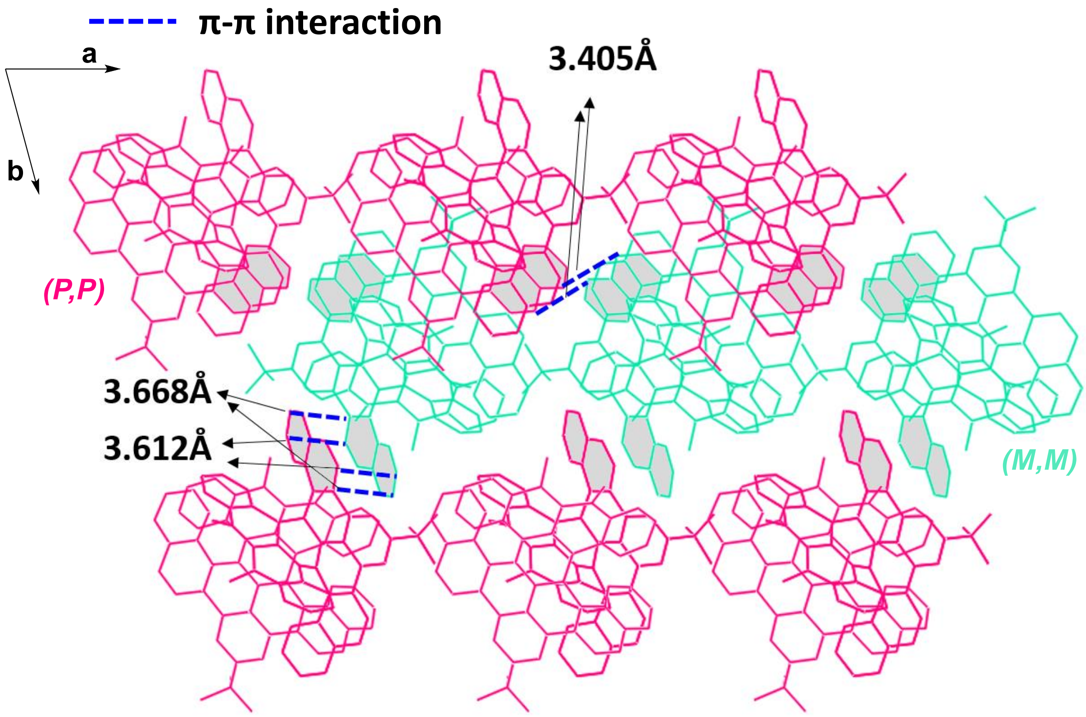

Figure S3 Intermolecular π -π interactions of **Naph-NBNDH**.

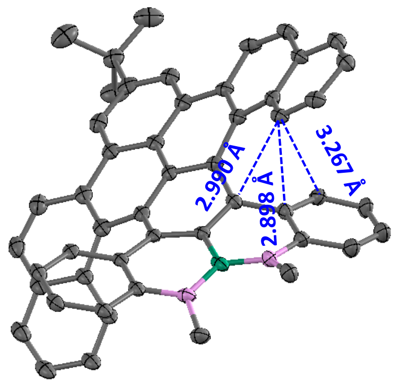

Figure S4 Intramolecular π -π interactions of **Naph-NBNDH**

Table S2 Crystal Data of **Naph-NBNDH** (CCDC: 1949281)

Empirical formula	$C_{107}H_{82}B_2N_4$
Formula weight	1445.38
Temperature/K	293(2)
Crystal system	triclinic
Space group	P-1
a/Å	13.1533(8)
b/Å	16.6236(10)
c/Å	17.7637(10)
α/°	87.371(5)

β/°	84.199(5)
γ/°	75.854(5)
Volume/Å^3	3746.2(4)
Z	2
ρ_{calc}g/cm^3	1.281
μ/mm^{-1}	0.558
F(000)	1524.0
Crystal size/mm^3	0.32 × 0.16 × 0.12
Radiation	CuKα (λ = 1.54184)
2Θ range for data collection/°	7.342 to 150.626
Index ranges	$-16 \leq h \leq 16$, $-20 \leq k \leq 20$, $-16 \leq l \leq 22$
Reflections collected	47690
Independent reflections	14800 [R_{int} = 0.2035, R_{sigma} = 0.2276]
Data/restraints/parameters	14800/0/1029
Goodness-of-fit on F^2	0.941
Final R indexes [I>=2σ (I)]	R_1 = 0.0890, wR_2 = 0.2118
Final R indexes [all data]	R_1 = 0.1898, wR_2 = 0.2704
Largest diff. peak/hole / e Å^{-3}	0.38/-0.43

3. Photophysical Properties

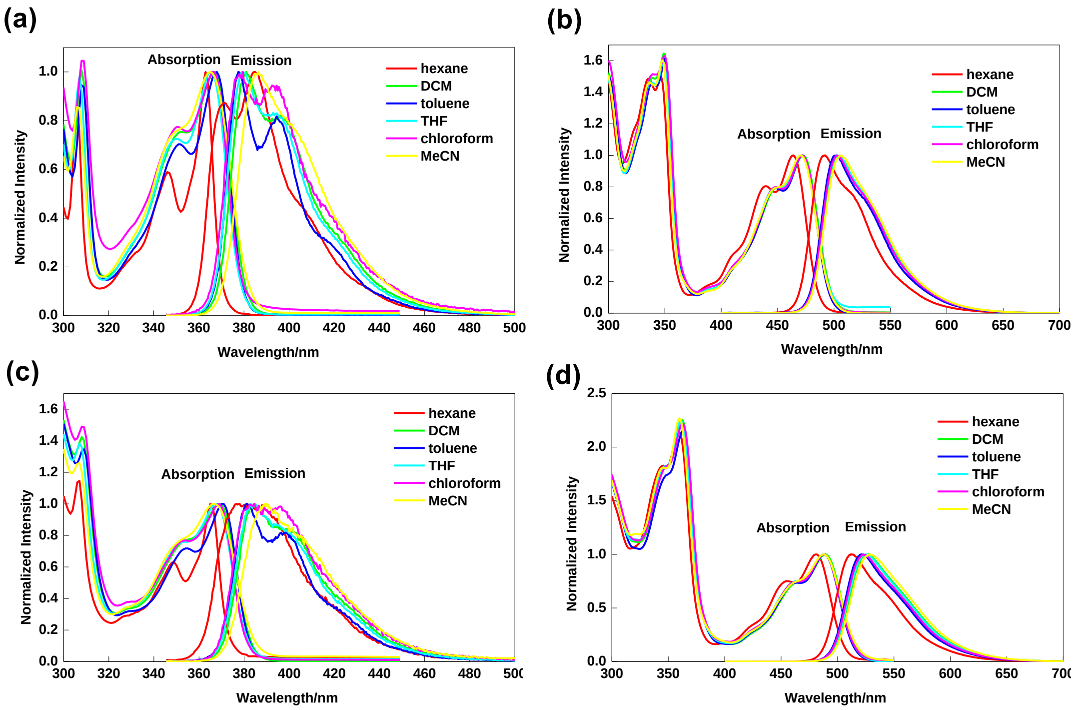

Figure S5 UV-vis Absorption and Fluorescence spectra of (a) **Ph-NBN**, (b) **Ph-NBNDH**, (c) **Naph-NBN**, (d) **Naph-NBNDH**; c = 2*10^{-5} M.

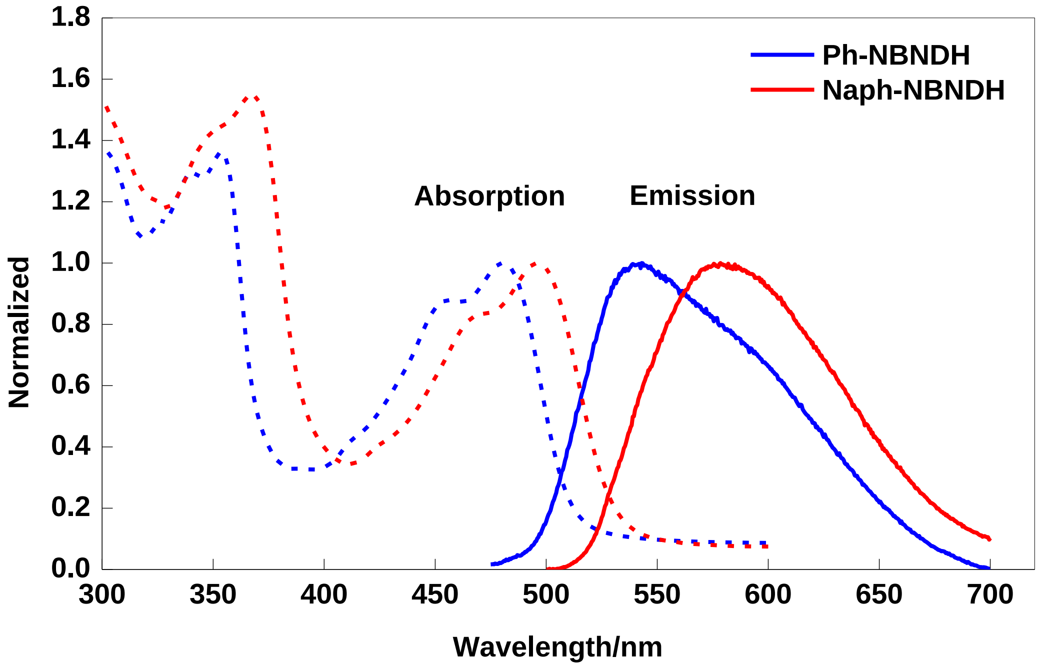

Figure S6 UV-vis Absorption（dotted line）and Fluorescence spectra (solid line) of film state. The absorption maxima: λ_{ab}= 481 nm for **Ph-NBNDH**, λ_{ab}= 496 nm for **Naph-NBNDH**; The emission maxima: λ_{em}= 543 nm for **Ph-NBNDH**, λ_{em}= 579 nm for **Naph-NBNDH**.

Table S3. Photophysical property data of **Ph-NBN**, **Ph-NBNDH**, **Naph-NBN** and **Naph-NBNDH** in DCM

Compound	absorption		fluorescence			Excited-state Dynamics		
	λ_{ab}(nm)	Log ε	λ_{em} (nm)	Φ_F in solutions	Φ_F in film	τ (ns)	k_r(s^{-1})	k_{nr}(s^{-1})
Ph-NBN	367	4.25	381	39%	/	3.6	$1.1*10^8$	$1.7*10^8$
Ph-NBNDH	473	4.41	505	83%	2.78%	6.4	$1.3*10^8$	$2.7*10^7$
Naph-NBN	369	4.26	384	7.4%	/	τ_1= 1.4 73.86% τ_2= 2.6 26.14%	$4.4*10^7$	$5.4 *10^8$
Naph-NBNDH	489	4.29	528	80%	2.48%	7.1	$1.1*10^8$	$2.8 *10^7$

Table S4. Performance comparison of our NBN-embedded double helicenes with the reported representative multiple helicenes. (λ_{em}: emission maxima; Φ_F: fluorescence quantum yields)

Compound	Isomers	λ_{em}/nm	Φ_F	Reference
Ph-NBNDH	*(P,P) or (M,M)*	505	0.83	Present work
Naph-NBNDH	*(P,P) or (M,M)*	528	0.80	

Double [6]carbohelicene 1	*(P,P) or (M,M)*	525	0.052	Ref S4(a)
	(P,M)	496	0.42	
Hexapole [5]carboheicene	*(P,M,P,P,M,P)*	517	0.041	Ref S4(b)
	(P,M,P,M,P,M)	513	0.039	
Double [7]carbohelicene 1	*(P,P) or (M,M)*	565	0.34	Ref S4(c)
	(P,M)	538	0.11	
Double [7]carbohelicene 2	*(P,P) or (M,M)*	697	0.035	Ref S4(d)
Quintuple [6]carboelicene	*(P,P,P,P,P) or (M,M,M,M,M)*	527, 553	0.03	Ref S4(e)
Double [6]carbohelicene 2	*(P,P)*	494	0.018	Ref S4(f)
Double [6]carbohelicene 3	*(P,P)*	434	0.041	
Hexapole [9]carboheicene	*(P,P,P,P,P,P) or (M,M,M,M,M)*	870	0.046	Ref S4(g)
Double [6]carbohelicene 4	*(P,P) or (M,M)*	529	0.75	Ref S4(h)
Hexapole [7]carboheicene	*(P,P,P,P,P,P) or (M,M,M,M,M)*	836, 934	0.016	Ref S4(i)
S-embedded double [6]helicene	*(P,P) or (M,M)*	524, 558	0.20	Ref S5(a)
S-embedded quadruple helicene	*(P,P)-(P,P)*	536, 570	0.017	Ref S5(b)
	(P,P)-(M,M)	514	0.11	
S-embedded quintuple [6]helicene	*(P,P,M,P,M)*	502, 534	0.02	Ref S5(g)
OBO-embedded double [5]helicene 1	*(P,P) or (M,M)*	430	0.68	Ref S5(c) Ref S5(d)
OBO-embedded double [5]helicene 2	*(P,P) or (M,M)*	436	0.65	
OBO-embedded double [5]helicene 3	*(P,P) or (M,M)*	490	0.03	Ref S5(e)
OBO-embedded double [7]helicene	*(P,P) or (M,M)*	487	0.036	Ref S5(f)
Imide-fused sixfold [5]helicene	*(P,P,P,P,P,P) or (M,M,M,M,M)*	617	0.24	Ref S5(h)
Imide-fused Se-embedded sixfold [5]helicene	*(P,P,P,P,P,P) or (M,M,M,M,M)*	617	0.06	
Imide-fused quintuple [6]elicene 1	*(P,P,P,P,P) or (M,M,M,M,M)*	/	0.0736	Ref S5(i)
Imide-fused quintuple [6]helicene 2	*(P,P,P,P,M) or (M,M,M,M,P)*	/	0.1185	
N-embedded double [6]helicene	*(P,P) or (M,M)*	454, 480	0.094	Ref S5(j)
N- embedded double [5]helicene	*(P,P) or (M,M)*	568	0.048	Ref S5(k)
Imide-fused double [6]helicene	*(P,P) or (M,M)*	549	0.44	Ref S5(l)

Imide-fused S-embedded double [6]helicene 1	*(P,P) or (M,M)*	726	0.025	Ref S5(m)
Imide-fused S-embedded double [6]helicene 2	*(P,P) or (M,M)*	726	0.031	

4. Electrochemical Properties

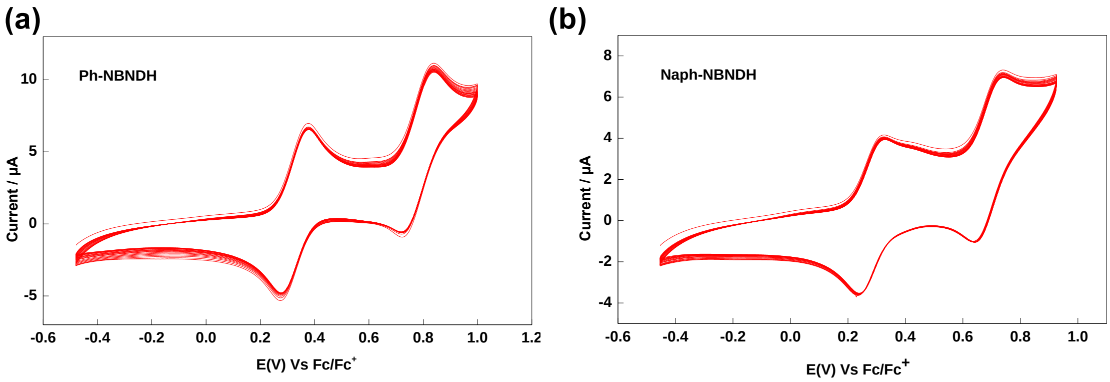

Figure S7 20-cycle cyclic voltammograms scans of (a) **Ph-NBNDH** and (b) **Naph-NBNDH** in dichloromethane containing 100 mM of $TBAPF_6$ at scan rate of 0.1V s^{-1}. Fc = ferrocene.

Table S5. Electrochemical data: redox peak vs ferrocene. The potentials evaluated by onset or (E_{ox}+E_{red})/2

Compumd	E^1/V	E^2/V
Ph-NBN	0.60	\
Ph-NBNDH	0.33	0.78
Naph-NBN	0.52	\
Naph-NBNDH	0.29	0.69

5. Electroluminescent device

Device fabrication and measurement of electroluminescence characteristics：

The OLED device was fabricated in the structure of ITO/MoO_3(5nm)/ Ph-NBNDH(65 nm)/Bphen (35 nm)/Liq(1nm)/Al (100 nm) employing ITO as the anode; MoO_3 as the hole injection layer; Ph-NBNDH as the emitting layer and hole transporting layer; 4,7-diphenyl-1,10-phenanthroline (Bphen) as the electron transporting layer; 8-hydroxy-quinolinato lithium (Liq) as the electron injection layer and Al as the cathode, respectively. The prepared ITO coated glass substrates were cleaned using detergent, de-ionized water, acetone, and isopropanol. After treated with a UV-ozone environment for 15 min, the substrate was immediately loaded into a custom-made high vacuum thermal evaporation chamber. The MoO_3 layer, the entire organic layers, and the Al cathode were successfully evaporated and deposited using shadow masks under a base pressure lower than 1.0×10^{-5} mbar. The deposition rates for MoO_3, organic materials, and Al were typically 0.3, 1.0 and 5.0 Å·s $^{-1}$, respectively. By this way, an OLEDs device with an active areas of 5 mm^2 was obtained. The electroluminescence characteristics were measured using a Keithley 2400 source meter and a PR650 Spectra Colorimeter under ambient condition at room temperature. The luminance and spectra were measured in the direction perpendicular to the substrate.

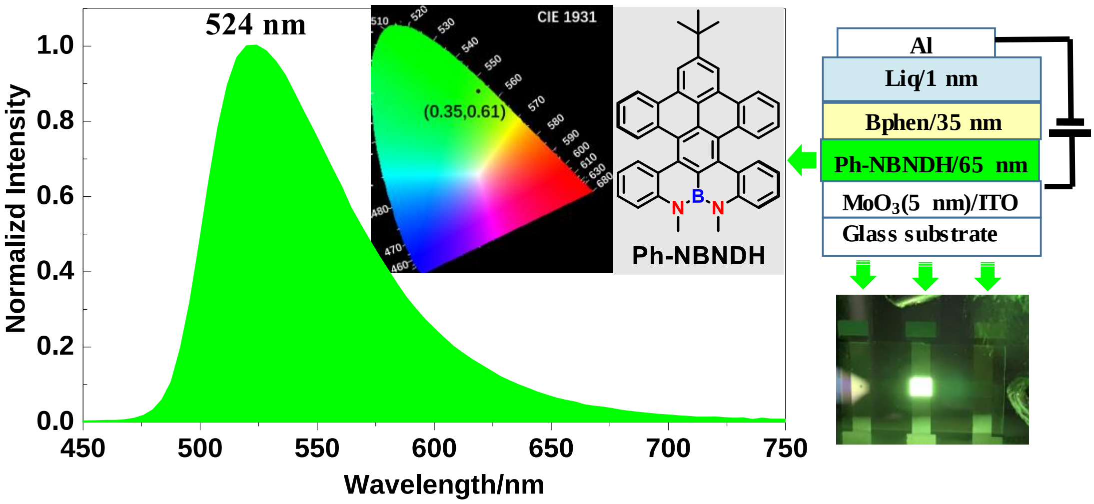

Figure S8 Electroluminescent (EL) device properties: the structure, luminescent spectra and CIE coordinate (inset). Bphen: 4,7-Diphenyl-1,10-phenanthroline.

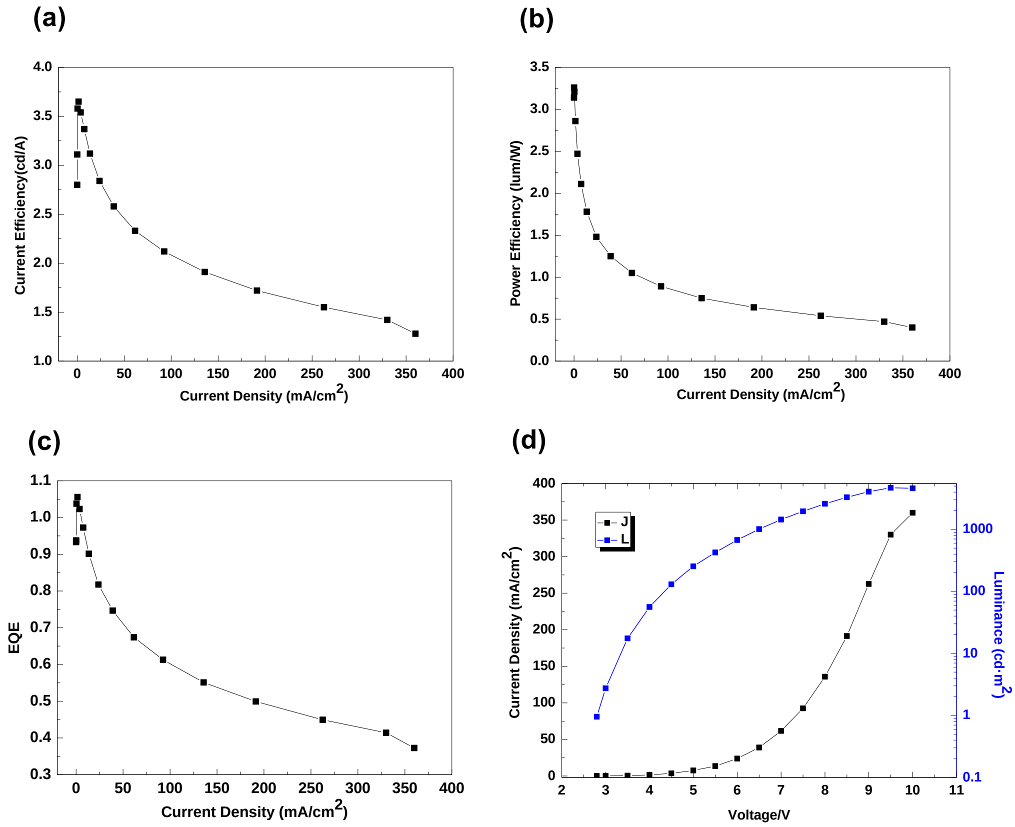

Figure S9 Electroluminescent (EL) device properties:(a) Current density-Current efficiency plots; (b) Current density-Power efficiency plots; (c) Current density-External quantum efficiency(EQE) plots; (d)voltage-current density(black line)/brightness plots (blue line)

Table S6 The performances of the Electroluminescent device with **Ph-NBNDH** as the host material

voltage (V)	L^a (cd/m^2)	η_c ^{b} (cd/A)	η_p ^{c} (lm/W)	EQE^d (%)	CIE x	y
2.8	0.95	2.80	3.14	0.93	0.36	0.59
4.0	55.98	3.65	2.86	1.06	0.36	0.60
9.5	4692	1.42	0.47	0.41	0.35	0.61

^{a}luminance; ^{b}current efficiency; ^{c}power efficiency; ^{d}external quantum efficiency.

6. Computational Studies

All density functional theory (DFT) calculation was performed using the Gaussian 09 program[S3]. The B3LYP functional with 6-31G(d) basis set were used for geometry optimization in the ground state. All geometry optimization was done in the gas phase and based on the single crystal structure. In order to simulate the UV-Vis spectra of the molecules TD-DFT calculations using B3LYP functional and 6-31G(d) basis set. For better comparison to the experimental absorption spectra the polarity of the solvent dichloromethane was added. The isomerization processes were calculated by nudged elastic band (NEB) method using Vienna ab initio Simulation Package (VASP).

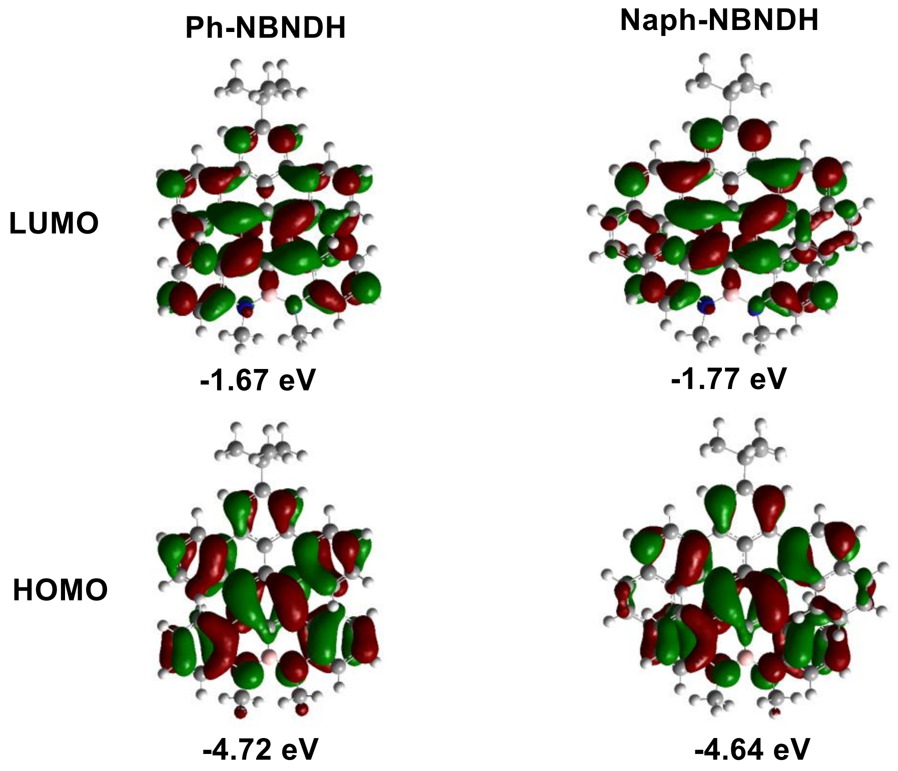

Figure S10 Calculated molecular orbitals of **Ph-NBNDH** and **Naph-NBNDH**

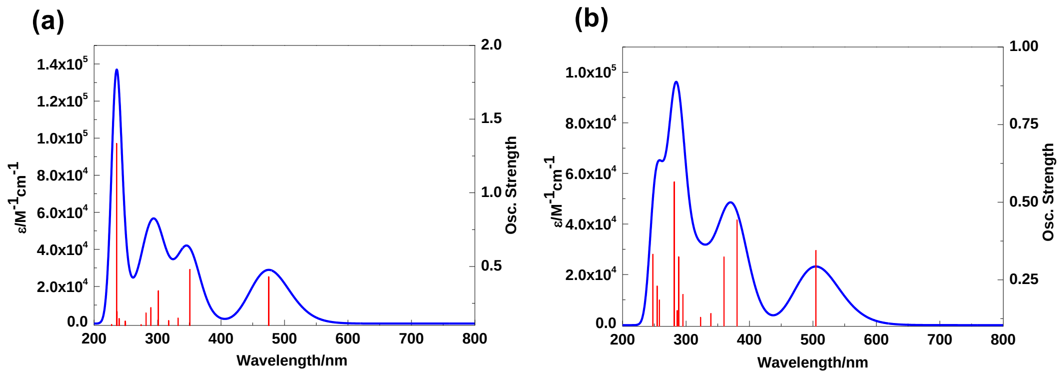

Figure S11 Simulated absorption spectra of (a) **Ph-NBNDH** and (b) **Naph-NBNDH**

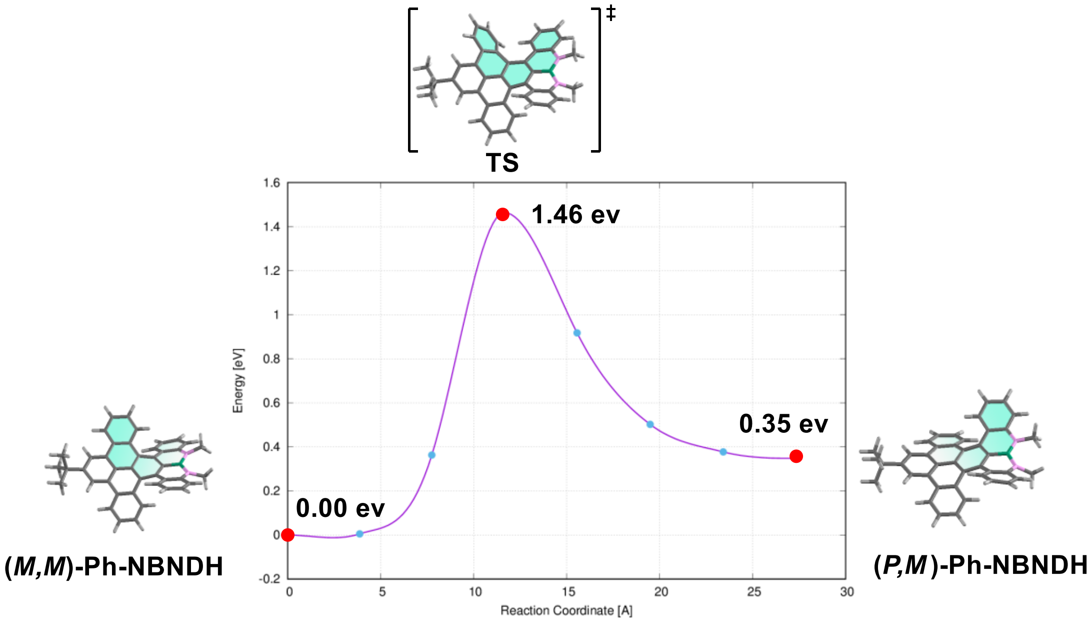

Figure S12 Calculated isomerization processes and relative internal energy of **Ph-NBNDH**

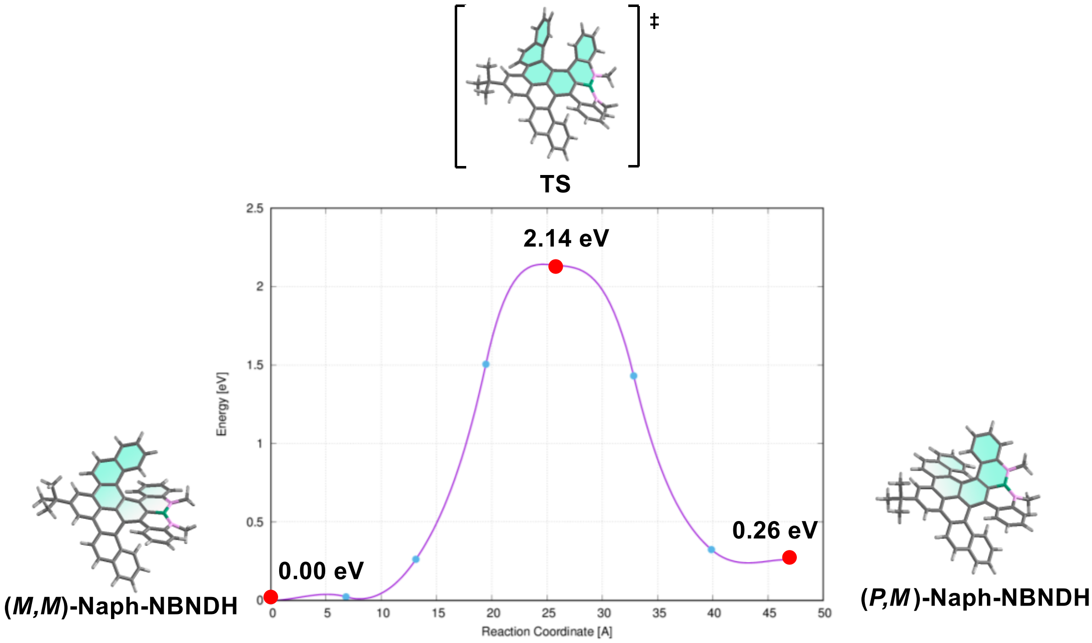

Figure S13 Calculated isomerization processes and relative internal energy of **Naph-NBNDH**

Table S7 Selected calculated wavelength, oscillator strength and compositions of major transitions of **Ph-NBNDH**.

Wavelength (nm)	Osc. Strength(*f*)	Major contribution
474.9	0.4295	HOMO->LUMO (99%)

350.7	0.4795	HOMO-2->LUMO (18%) HOMO-1->LUMO (36%) HOMO->LUMO+1 (33%)

Table S8 Selected calculated wavelength, oscillator strength and compositions of major transitions of **Naph-NBNDH**.

Wavelength (nm)	**Osc. Strength(*f*)**	**Major contribution**
504.4	0.3441	HOMO->LUMO (98%)
380.2	0.4426	HOMO-3->LUMO (20%) HOMO-2->LUMO (56%) HOMO->LUMO+1 (13%)

Appendix: Cartesian coordinatesfor DFTcalculations

(*M,M*)-Ph-NBNDH:

Tag	Symbol	X	Y	Z
1	N	-4.44018	1.24075	0.13716
2	C	-3.74632	2.33584	0.68013
3	B	-3.75921	-0.0211	-0.00289
4	C	-3.79037	4.48638	1.82905
5	H	-4.36529	5.31325	2.2376
6	N	-4.41999	-1.29346	-0.14425
7	C	-4.45199	3.4378	1.20313
8	H	-5.53463	3.45472	1.1569
9	C	-2.39962	4.45462	1.96362
10	H	-1.87541	5.24808	2.48819
11	C	-1.69087	3.39091	1.42594
12	H	-0.61298	3.36186	1.53572
13	C	-2.32162	2.33646	0.73423
14	C	-1.54655	1.21441	0.18512
15	C	-2.22484	-0.00893	-0.00153
16	C	-1.5267	-1.22215	-0.18589
17	C	-2.28319	-2.35675	-0.73545
18	C	-2.32546	-4.47728	-1.96252
19	H	-1.78772	-5.26324	-2.48468
20	C	-1.63455	-3.40219	-1.42418
21	H	-0.55694	-3.35676	-1.53117
22	C	-3.71592	-4.53	-1.83196
23	H	-4.27707	-5.36589	-2.24131

24	C	-4.39517	-3.49094	-1.20904
25	H	-5.47756	-3.52428	-1.16586
26	C	-3.70783	-2.37796	-0.68497
27	C	-5.79043	-1.54674	0.29928
28	H	-5.83254	-2.49665	0.84308
29	H	-6.51376	-1.59727	-0.52606
30	H	-6.10073	-0.75655	0.98285
31	C	-5.8133	1.47279	-0.30964
32	H	-6.53916	1.51311	0.51404
33	H	-6.11002	0.67728	-0.99307
34	H	-5.86866	2.42143	-0.85449
35	C	1.97475	2.4046	-0.72835
36	C	2.62682	3.52955	-1.28285
37	H	3.70734	3.53979	-1.36613
38	C	1.92177	4.61491	-1.77062
39	H	2.45428	5.46084	-2.19686
40	C	0.5198	4.59454	-1.74898
41	H	-0.04906	5.41737	-2.17344
42	C	-0.1418	3.50967	-1.20503
43	H	-1.22378	3.49108	-1.22271
44	C	0.55658	2.41236	-0.64584
45	C	-0.155	1.24322	-0.12551
46	C	0.55464	0.01242	0.00258
47	C	2.00341	0.02322	0.00171
48	C	2.71687	1.21279	-0.31103
49	C	4.12093	1.19725	-0.28217
50	H	4.65364	2.11467	-0.48725
51	C	4.85261	0.04304	-0.00799
52	C	4.13363	-1.12323	0.27242
53	H	4.68663	-2.03223	0.47412
54	C	2.73511	-1.1597	0.31167
55	C	2.00895	-2.3606	0.73428
56	C	0.59158	-2.38794	0.65174
57	C	-0.13661	-1.22932	0.12872
58	C	2.67673	-3.47305	1.29377
59	H	3.75724	-3.46614	1.37874
60	C	1.98696	-4.56707	1.78489
61	H	2.53115	-5.40351	2.21505
62	C	0.58511	-4.56692	1.76151
63	H	0.0276	-5.39648	2.18792
64	C	-0.09159	-3.493	1.21371
65	H	-1.17378	-3.48966	1.23034
66	C	6.39271	0.01162	-0.00539
67	C	7.01047	1.38494	-0.33142

68	H	8.10368	1.3098	-0.3169
69	H	6.7234	2.14694	0.40218
70	H	6.71809	1.73909	-1.3266
71	C	6.88812	-1.00046	-1.06588
72	H	7.98449	-1.03755	-1.07393
73	H	6.54965	-0.71477	-2.06832
74	H	6.52291	-2.01344	-0.86693
75	C	6.89879	-0.42139	1.39129
76	H	7.99508	-0.45653	1.40529
77	H	6.5303	-1.41436	1.6693
78	H	6.57094	0.28424	2.16308

(*M*,*M*)-Naph-NBNDH:

Tag	Symbol	X	Y	Z
1	N	4.2267	1.33601	-0.37268
2	N	4.2964	-1.09882	0.39741
3	C	-2.83462	-1.31904	0.04571
4	C	0.00271	-3.68904	-0.74383
5	C	1.33971	1.20332	-0.37573
6	C	-0.71426	-0.02839	-0.00155
7	C	-0.81707	2.45292	0.21082
8	C	-2.90711	1.13753	-0.0538
9	C	-0.67091	-2.50893	-0.22126
10	C	-4.99578	-0.15536	0.00588
11	C	-2.15261	-0.07102	-0.00344
12	C	2.06198	0.05272	0.00468
13	C	-2.72005	-3.83344	-0.05455
14	H	-3.77352	-3.89656	0.18987
15	C	-2.0692	-2.56008	-0.05314
16	C	-0.21641	3.6739	0.72804
17	C	-0.68542	-4.94237	-0.75223
18	C	1.40712	-1.13797	0.3808
19	C	-2.21437	2.42236	0.0356
20	C	0.02354	-1.25335	0.04637
21	C	-4.24033	-1.32545	0.06009
22	H	-4.75835	-2.2728	0.08109
23	C	-2.044	-4.98638	-0.32996
24	H	-2.55435	-5.94587	-0.29538
25	C	2.06403	2.23664	-1.12613
26	C	3.48837	2.28614	-1.10359
27	C	-4.30584	1.05947	-0.05726
28	H	-4.88362	1.97446	-0.07217
29	C	-0.04896	1.23789	-0.0479
30	C	2.18613	-2.12795	1.13449

31	C	-0.03532	-6.10636	-1.23258
32	H	-0.5754	-7.05004	-1.20389
33	C	1.28912	-3.65382	-1.34344
34	H	1.80101	-2.70557	-1.44431
35	C	-2.93781	3.65523	0.02022
36	H	-3.99088	3.65438	-0.23422
37	C	1.55681	-3.07899	1.96106
38	H	0.47461	-3.07325	2.02278
39	C	-2.3313	4.84802	0.28841
40	H	-2.89519	5.77642	0.23999
41	C	3.61103	-2.09234	1.12197
42	C	1.59267	4.89522	1.82836
43	H	2.5705	4.88648	2.30247
44	C	-0.97581	4.88568	0.72044
45	C	1.06553	3.71837	1.33647
46	H	1.63103	2.8024	1.44949
47	C	-6.53679	-0.1573	0.01653
48	C	1.38497	3.14574	-1.96036
49	H	0.30558	3.07454	-2.03002
50	C	1.23542	-6.04184	-1.76045
51	H	1.72082	-6.93745	-2.13883
52	C	1.88659	-4.79369	-1.84209
53	H	2.86531	-4.72426	-2.3093
54	C	2.27382	-4.00963	2.6983
55	H	1.75153	-4.7265	3.32501
56	C	-0.3971	6.08952	1.19399
57	H	-0.99044	7.00016	1.15308
58	C	0.8713	6.10309	1.73087
59	H	1.30167	7.02847	2.10414
60	C	-7.06313	0.52108	-1.27066
61	H	-6.7193	1.55697	-1.35757
62	H	-8.16002	0.53319	-1.27411
63	H	-6.72621	-0.01798	-2.1634
64	C	4.14931	3.29182	-1.83445
65	H	5.23189	3.34267	-1.82381
66	C	4.32586	-3.05829	1.85573
67	H	5.4096	-3.04403	1.85296
68	C	2.05025	4.11602	-2.69504
69	H	1.49056	4.79855	-3.32777
70	C	3.6689	-4.00775	2.6287
71	H	4.25026	-4.7299	3.19591
72	C	-7.1251	-1.57993	0.07896
73	H	-6.83157	-2.18268	-0.78808
74	H	-8.21943	-1.52428	0.08595

75	H	-6.8165	-2.11036	0.98705
76	C	3.44229	4.19836	-2.6148
77	H	3.98345	4.95289	-3.17961
78	C	5.68251	-1.3822	0.02591
79	H	6.39309	-1.24318	0.85212
80	H	5.97722	-0.73014	-0.79633
81	H	5.7668	-2.41786	-0.32049
82	C	-7.04353	0.62413	1.25244
83	H	-6.69187	0.15986	2.18079
84	H	-8.14026	0.63684	1.27229
85	H	-6.69934	1.66363	1.24903
86	B	3.59573	0.09881	0.01008
87	C	5.5918	1.70032	0.00545
88	H	6.31297	1.60514	-0.81787
89	H	5.92116	1.06522	0.82781
90	H	5.61339	2.73864	0.35364

7. Optical Resolution of Naph-NBNDH

Preparative Seperation Method

Instrument: MG II preparative SFC (SFC-11)

Column: ChiralPak AD, 250×30mm I.D., 5μm

Mobile phase: A for CO_2 and B for Ethanol(0.1%NH3H2O)

Gradient: B 40%

Flow rate: 70 mL /min

Back pressure: 100 bar

Column temperature: 38℃

Wavelength: 220nm

Cycle time: ~10min

Analytical separation method:

Instrument: Waters UPC2 analytical SFC (SFC-H)

Column: ChiralPak AD, 150×4.6mm I.D., 3μm

Mobile phase: A for CO_2 and B for Ethanol (0.05%DEA)

Gradient: B 40%

Flow rate: 2.5 mL/min

Back pressure: 100 bar

Column temperature: 35℃

Wavelength: 220nm

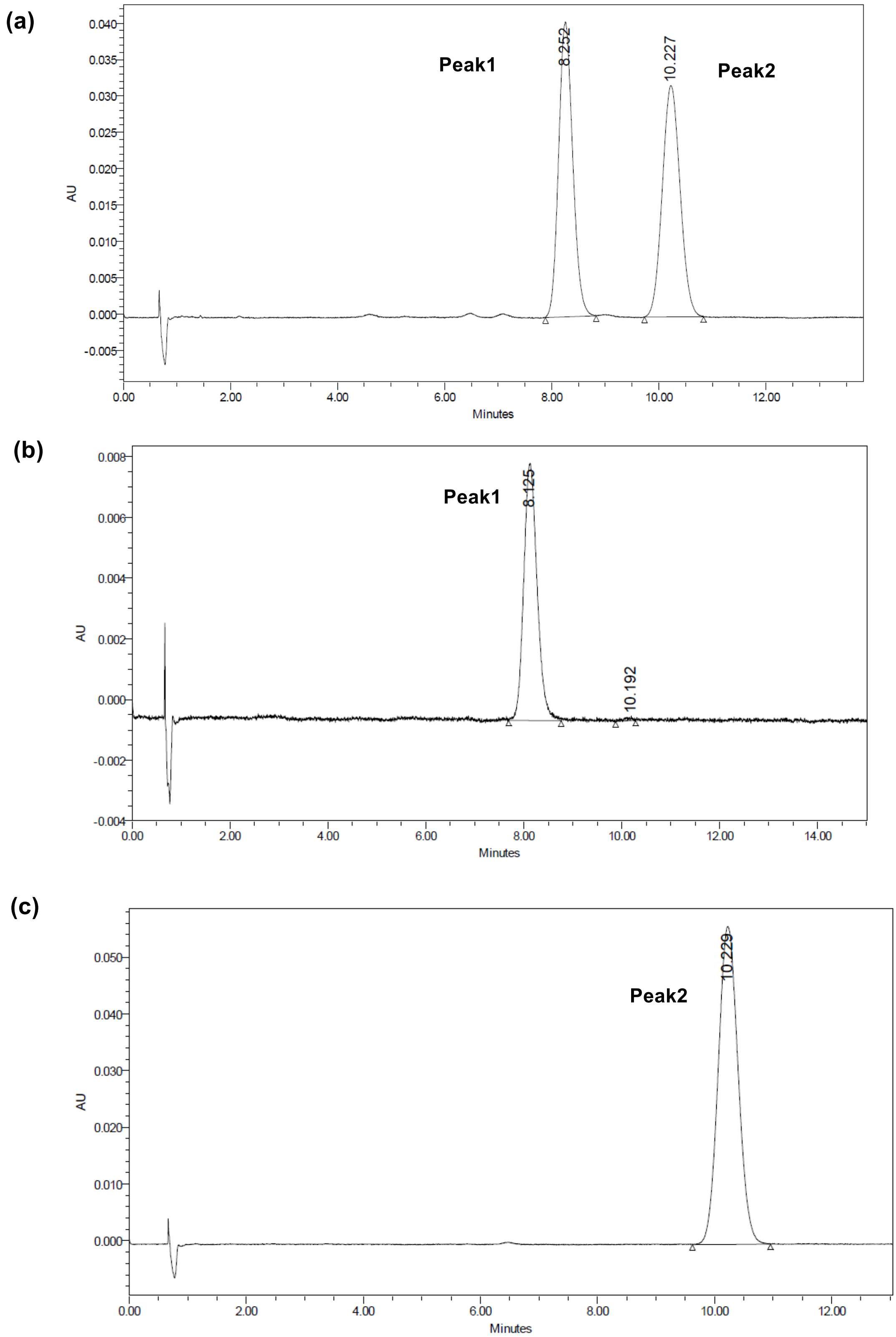

Figure S14 Chiral SCF profiles of (a) rac-**Naph-NBNDH**, (b) Peak1-**Naph-NBNDH**, and (c) Peak2-**Naph-NBNDH**.

Table S9 The SCF profiles of **Naph-NBNDH**

	Fraction	Retention Time /min	Area	Area%	ee
rac Form	Peak 1	8.252	743073	50.18	
	Peak 2	10.227	737734	49.82	
Peak 1	Peak 1	8.125	160691	99.19	98.38
	Peak 2	10.192	1307	0.81	
Peak 2	Peak 1	0	0	0	100%
	Peak 2	10.229	1320204	100.00	

8. NMR Spectra and HRMS Spectra

^{1}H NMR spectrum of **1** (400 M Hz, $CDCl_3$)

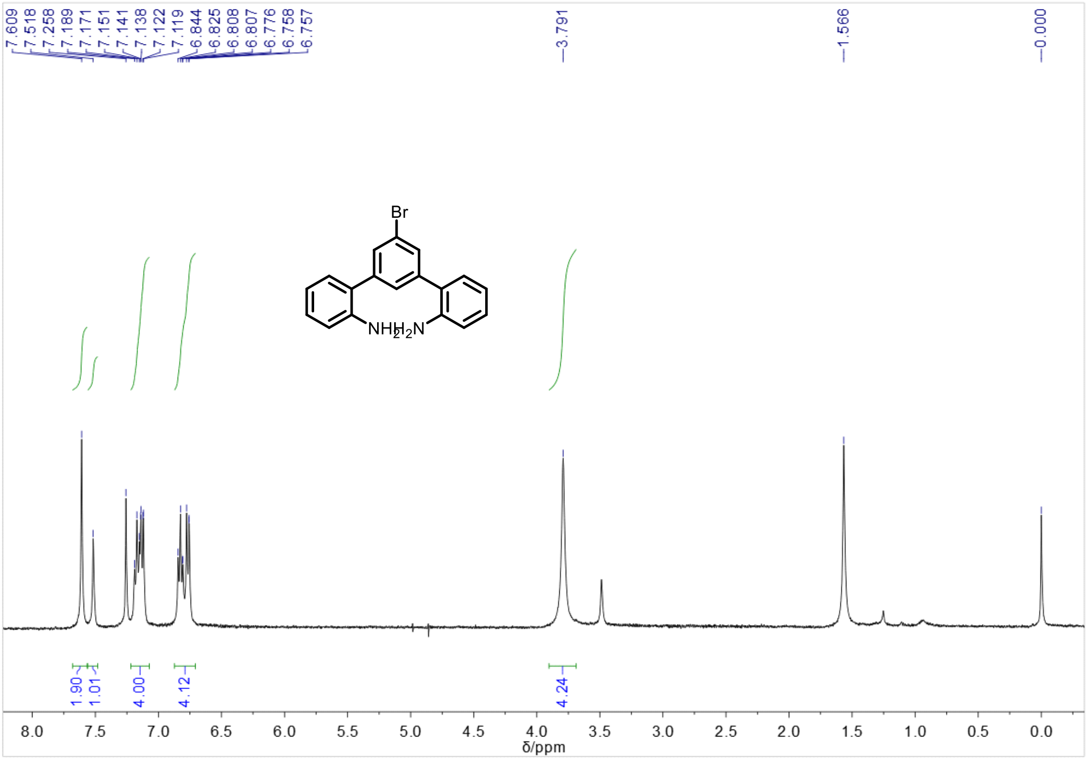

^{13}C NMR spectrum of **1** (125 M Hz, $CDCl_3$)

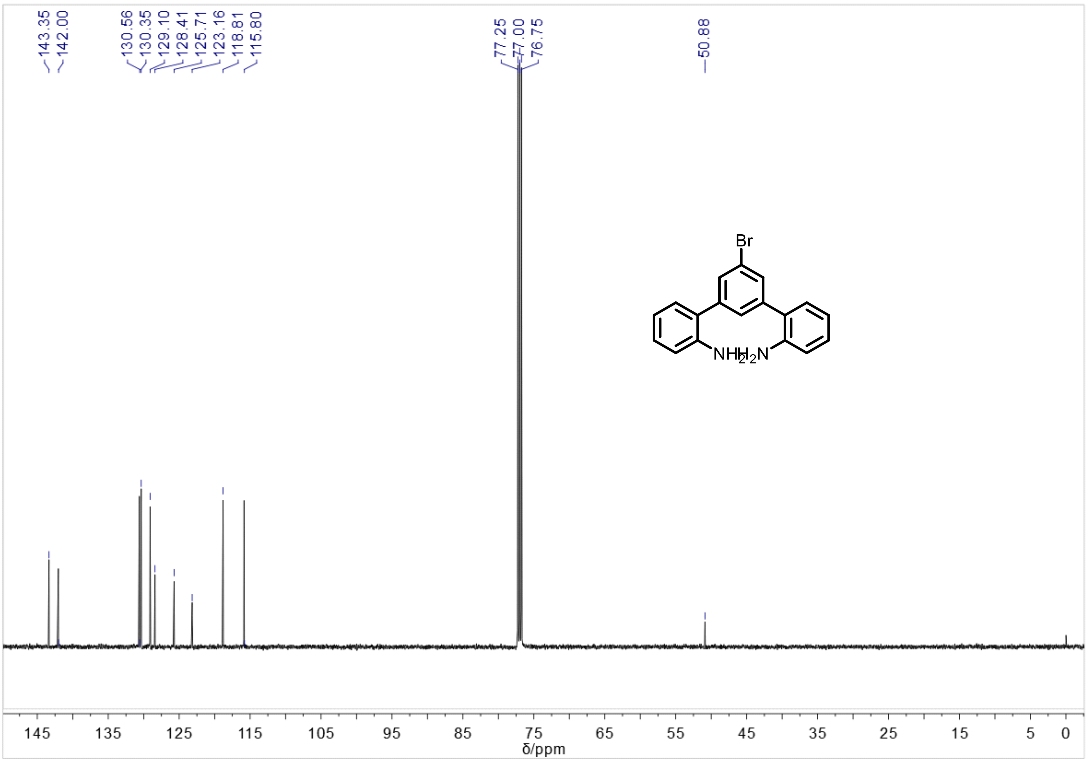

HRMS (ESI-MS) spectra of **1**

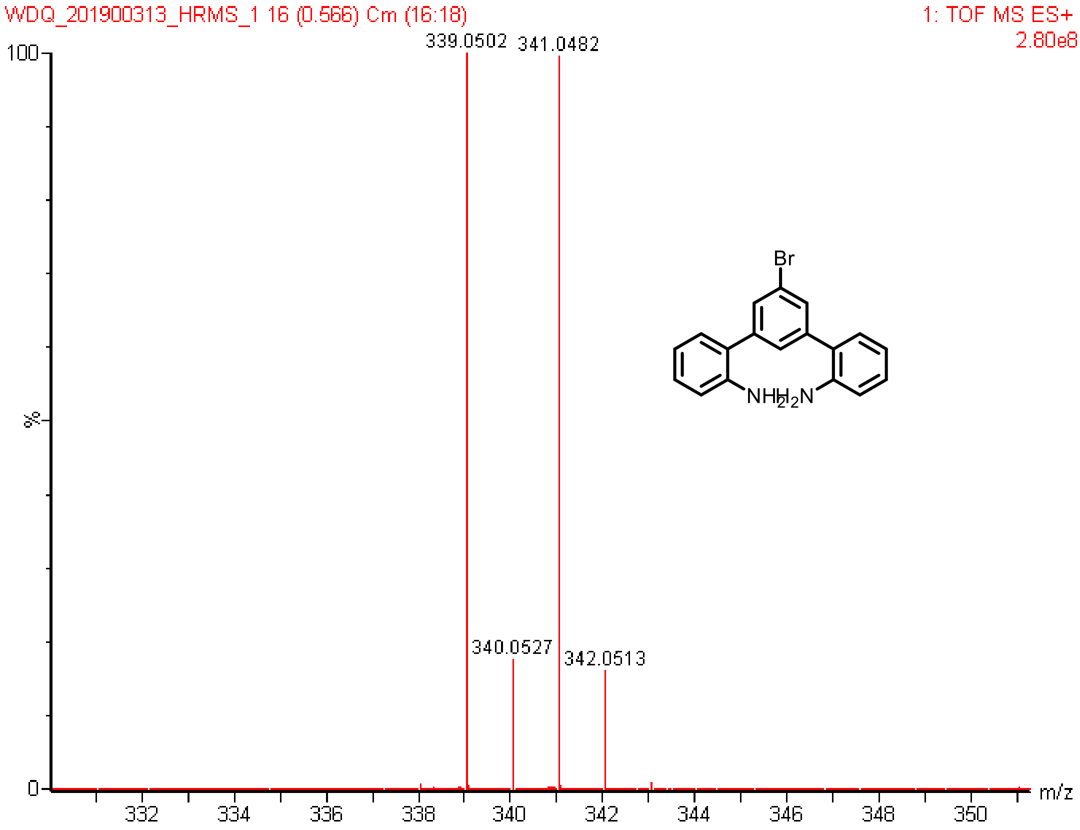

^{1}H NMR spectrum of **2** (500 M Hz, $CDCl_3$)

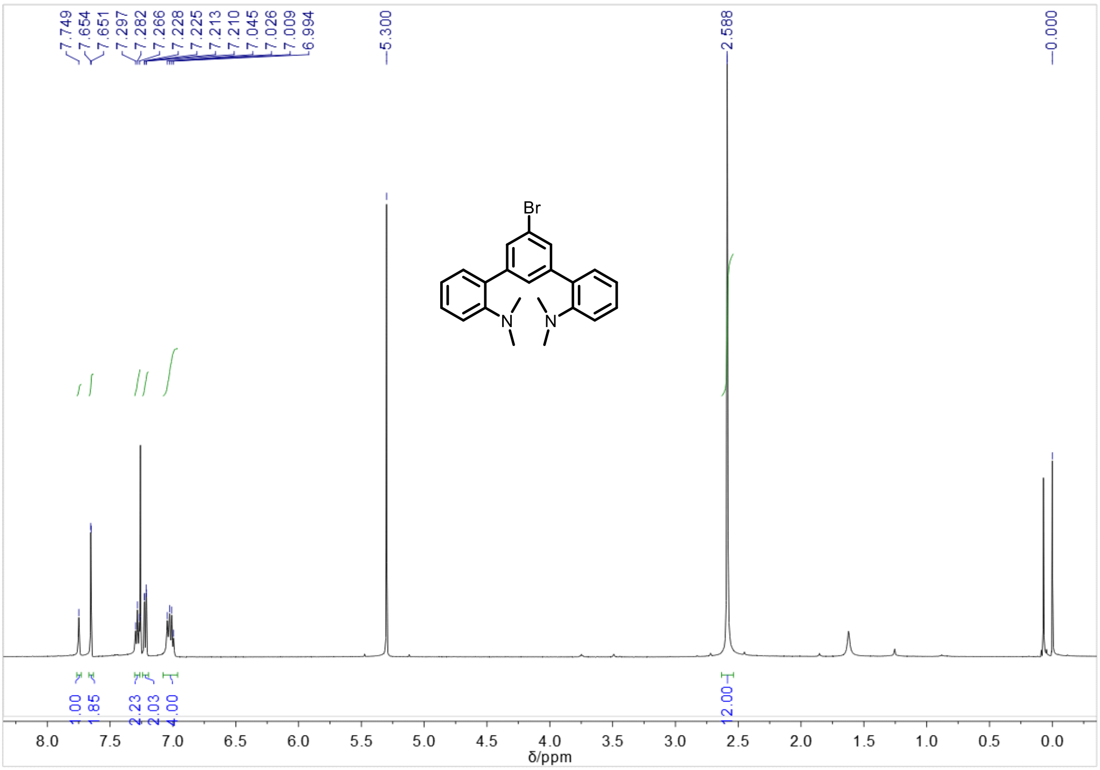

^{13}C NMR spectrum of **2** (125 M Hz, $CDCl_3$)

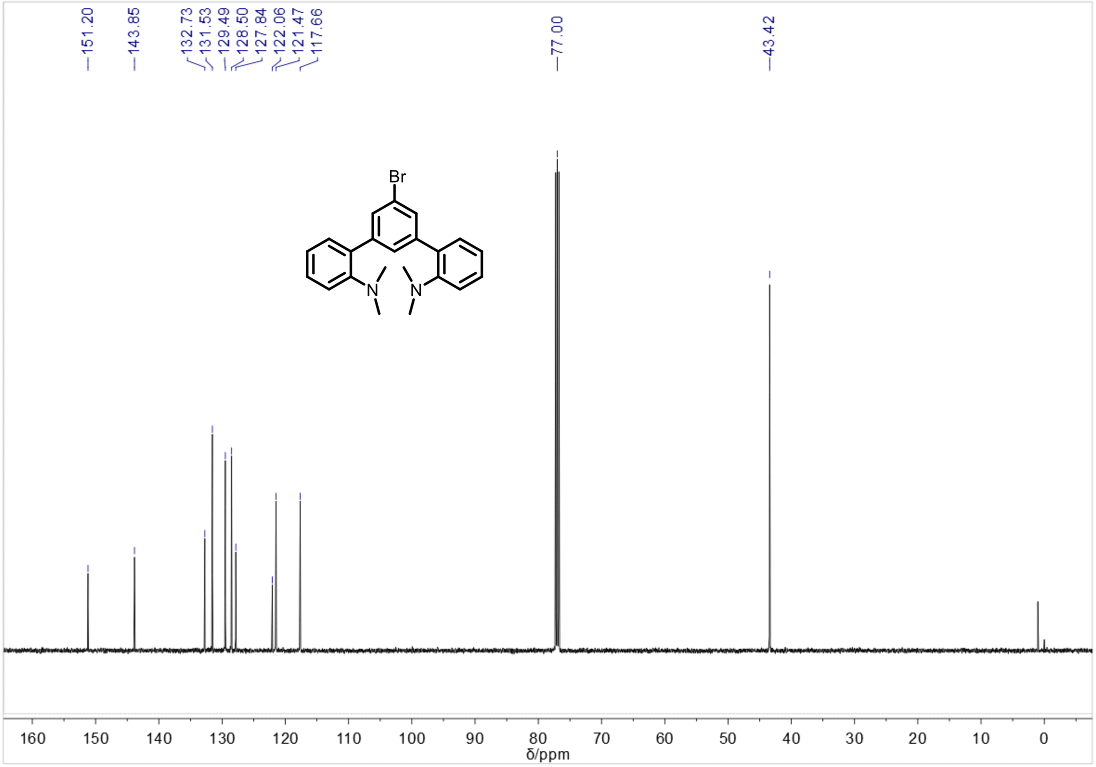

HRMS (ESI-MS) spectra of **2**

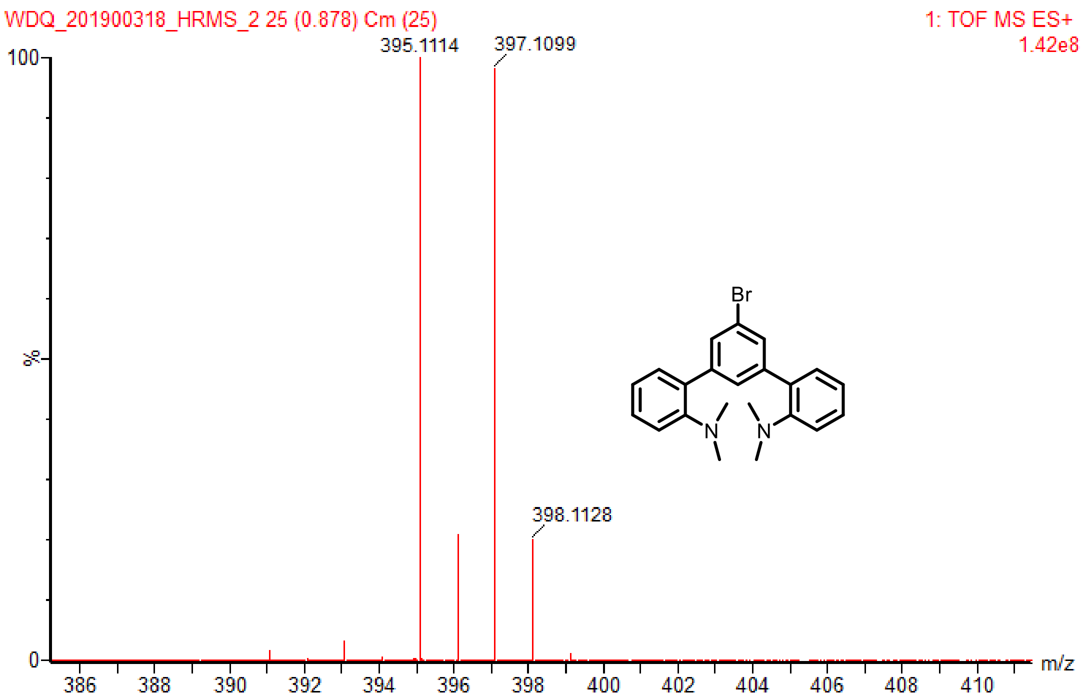

^{1}H NMR spectrum of **Br-NBNDH** (500 M Hz, $CDCl_3$)

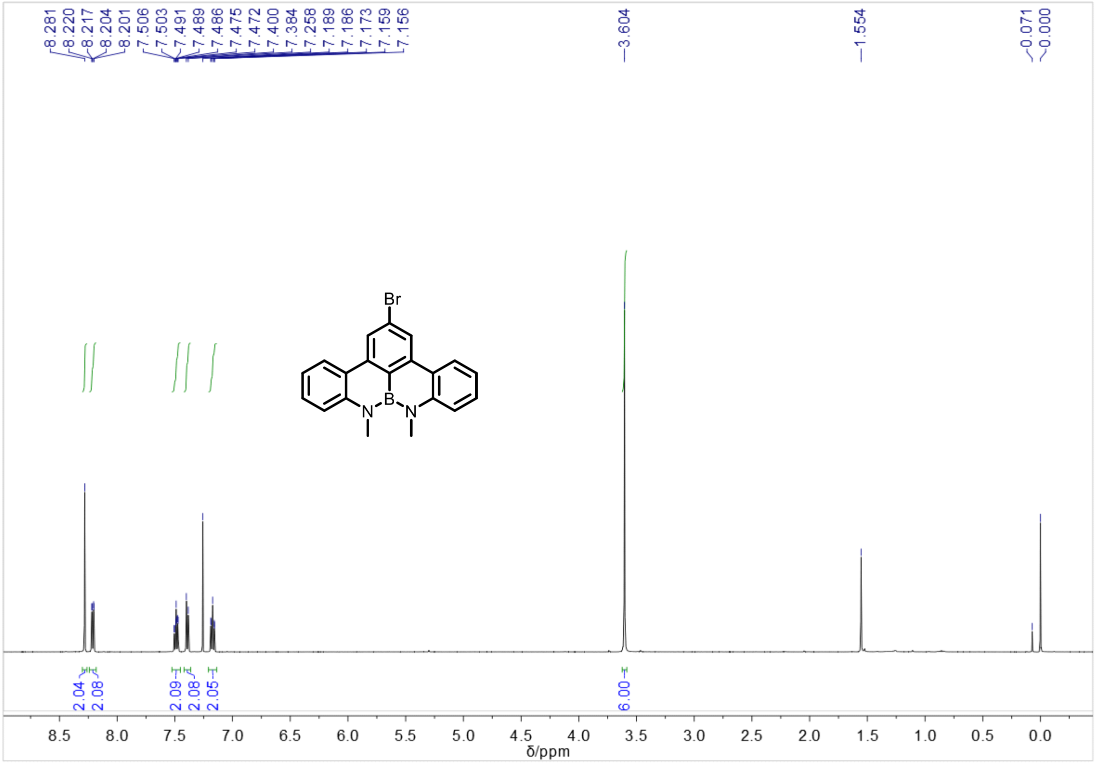

^{13}C NMR spectrum of **Br-NBN** (100 M Hz, $CDCl_3$)

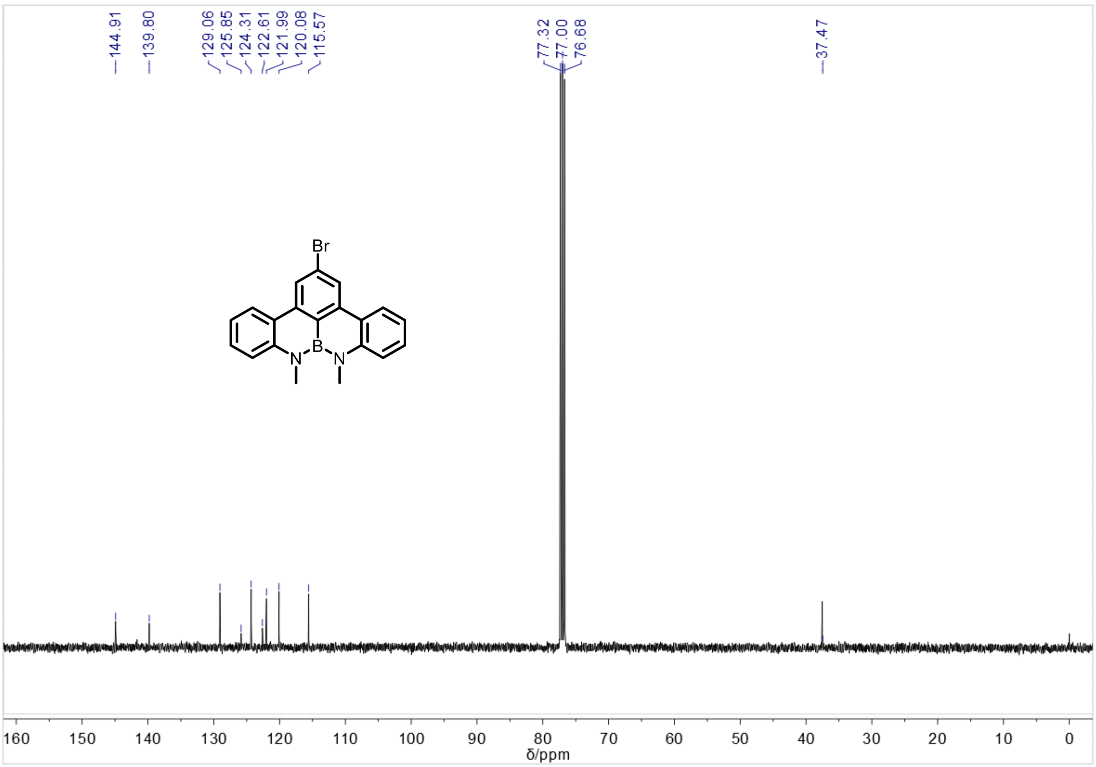

^{11}B NMR spectrum of **Br-NBN** (128 M, $CDCl_3$)

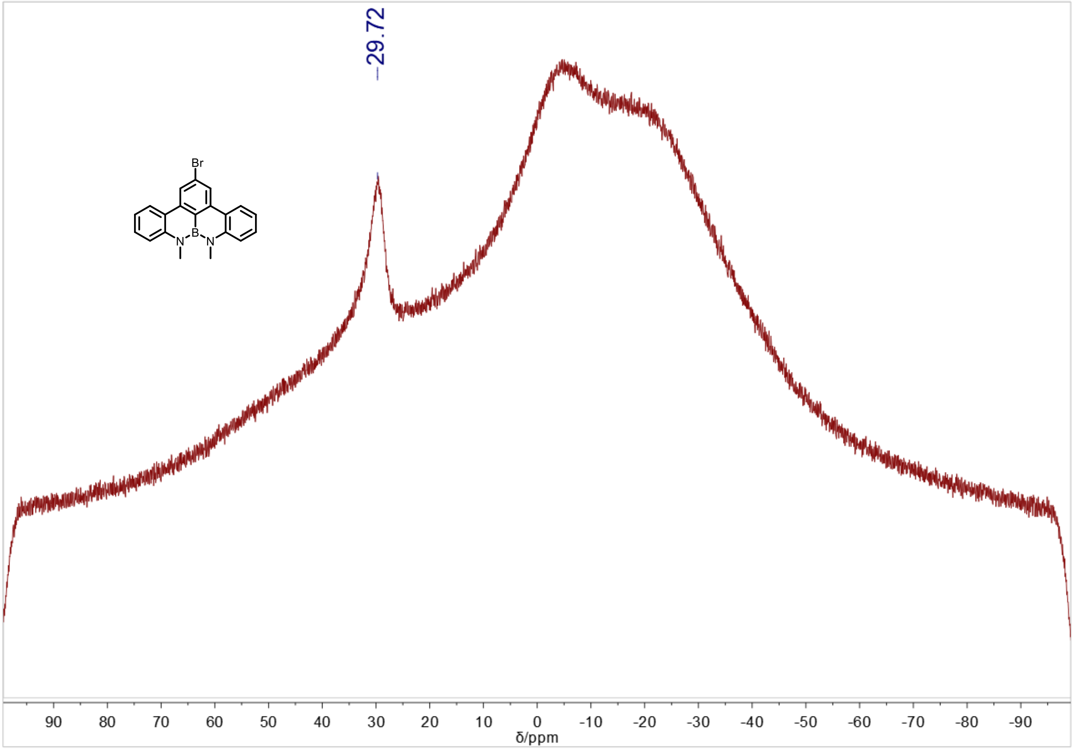

HRMS (ESI-MS) spectra of **Br-NBN**

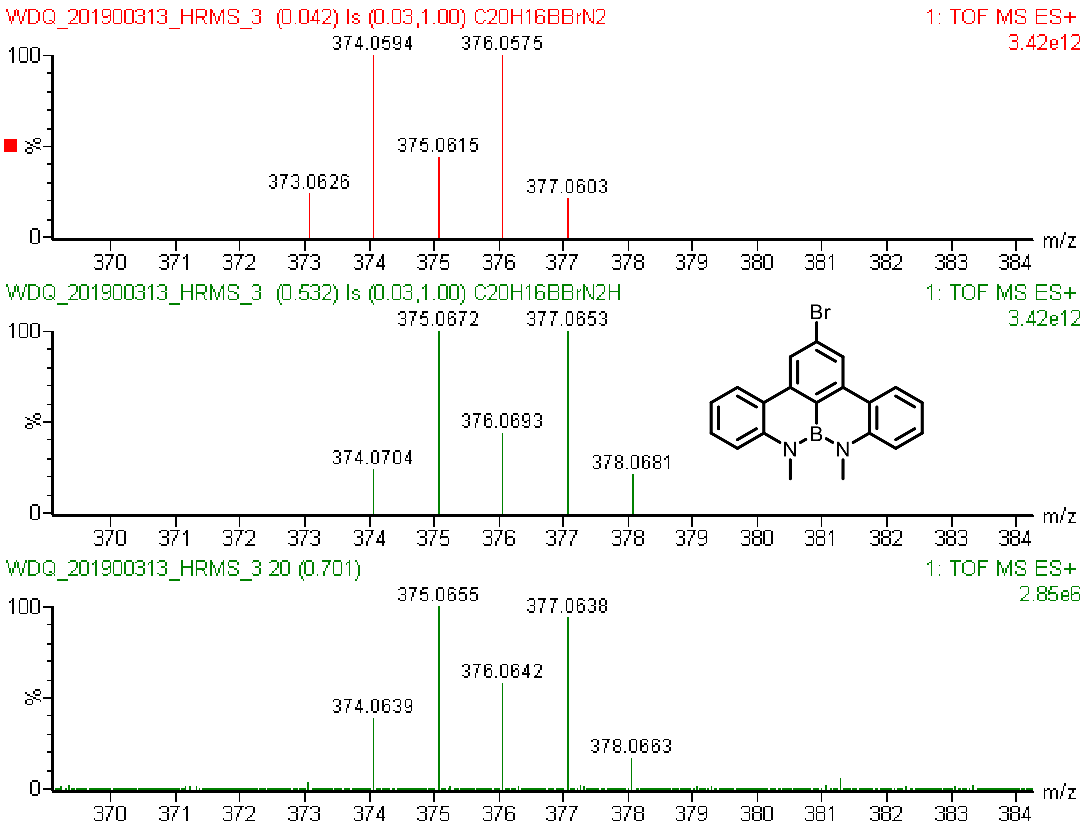

[1]H NMR spectrum of **3** (400 M Hz, $CDCl_3$)

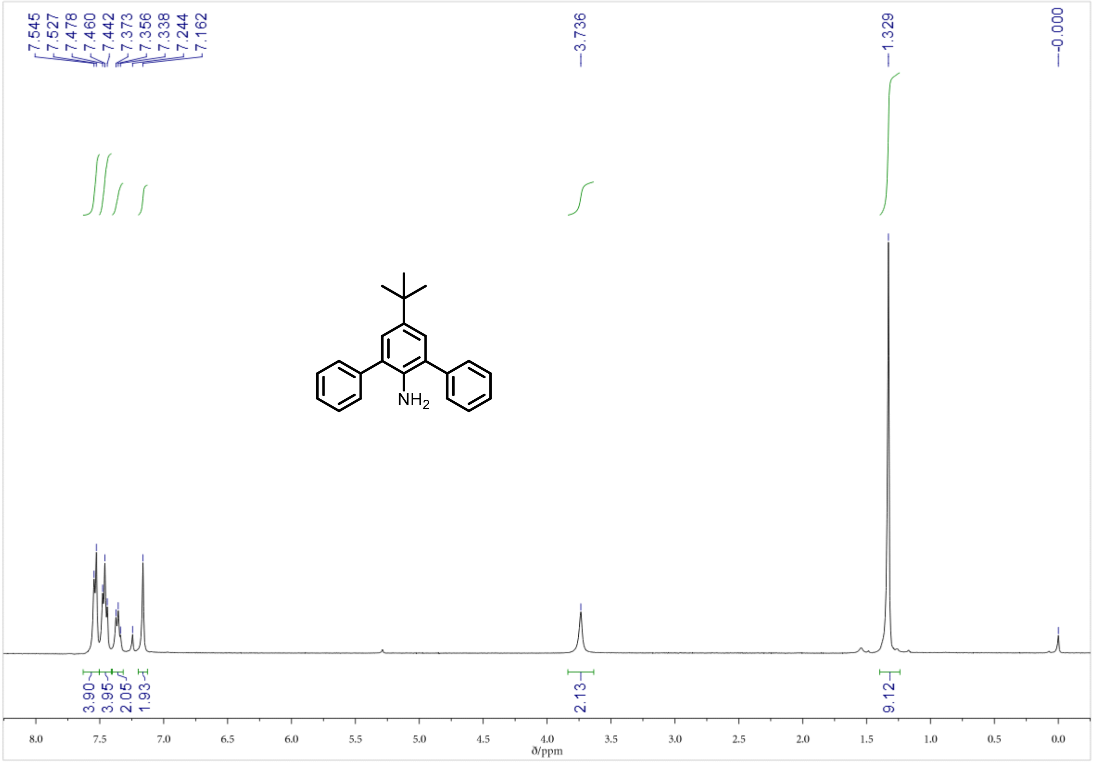

[13]C NMR spectrum of **3** (125 M Hz, $CDCl_3$)

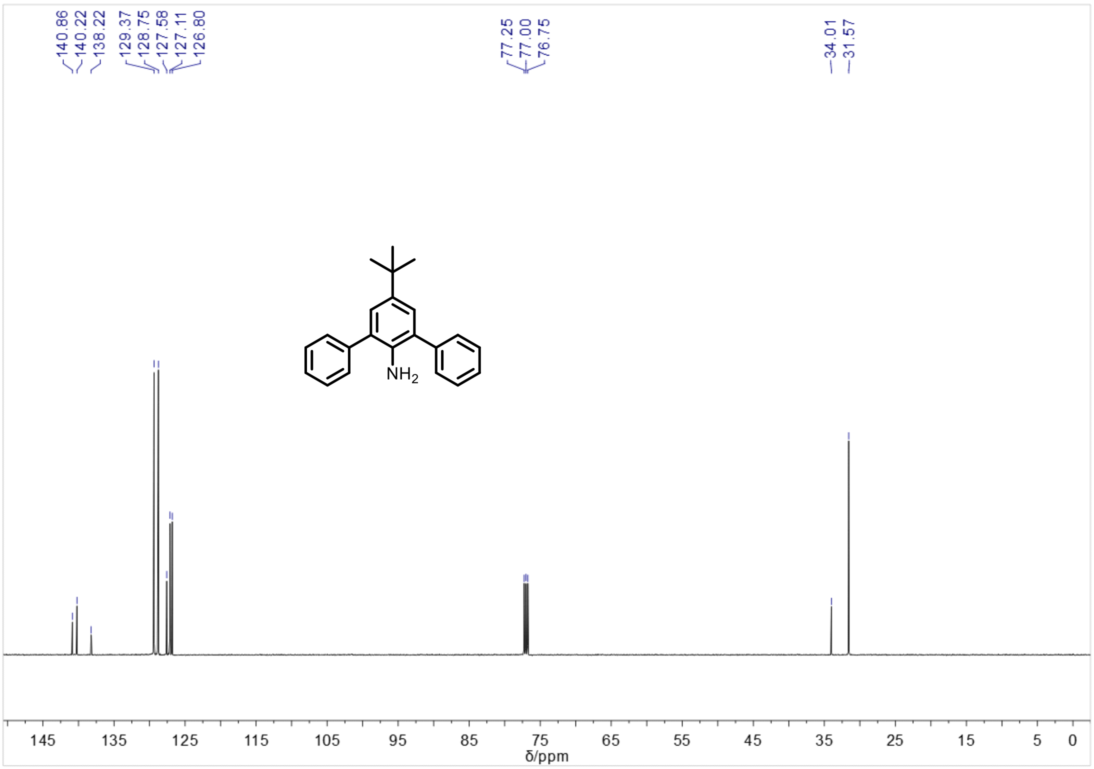

MALDI-FTICR spectra of **3**

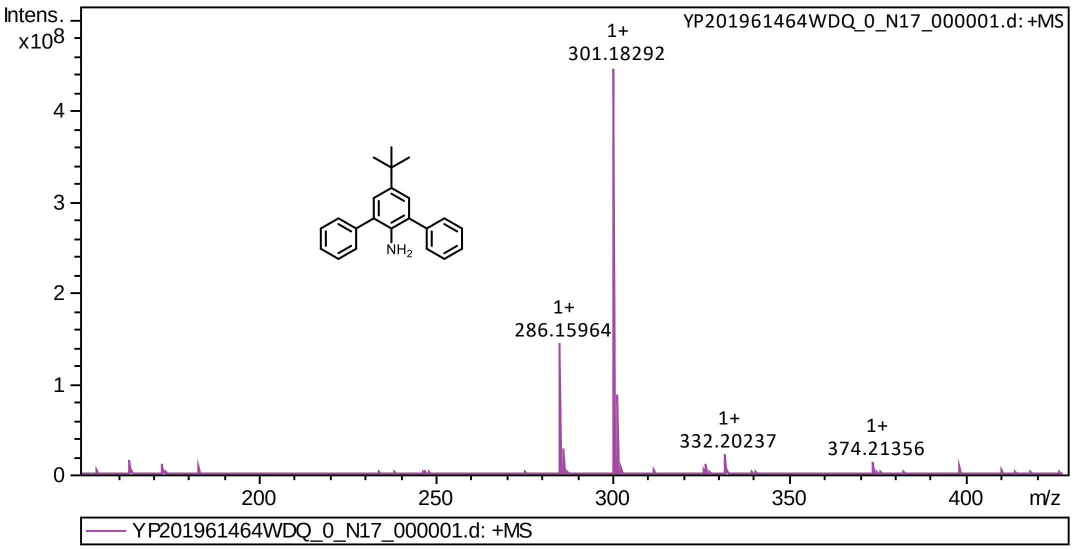

^{1}H NMR spectrum of **5** (500 M Hz, $CDCl_3$)

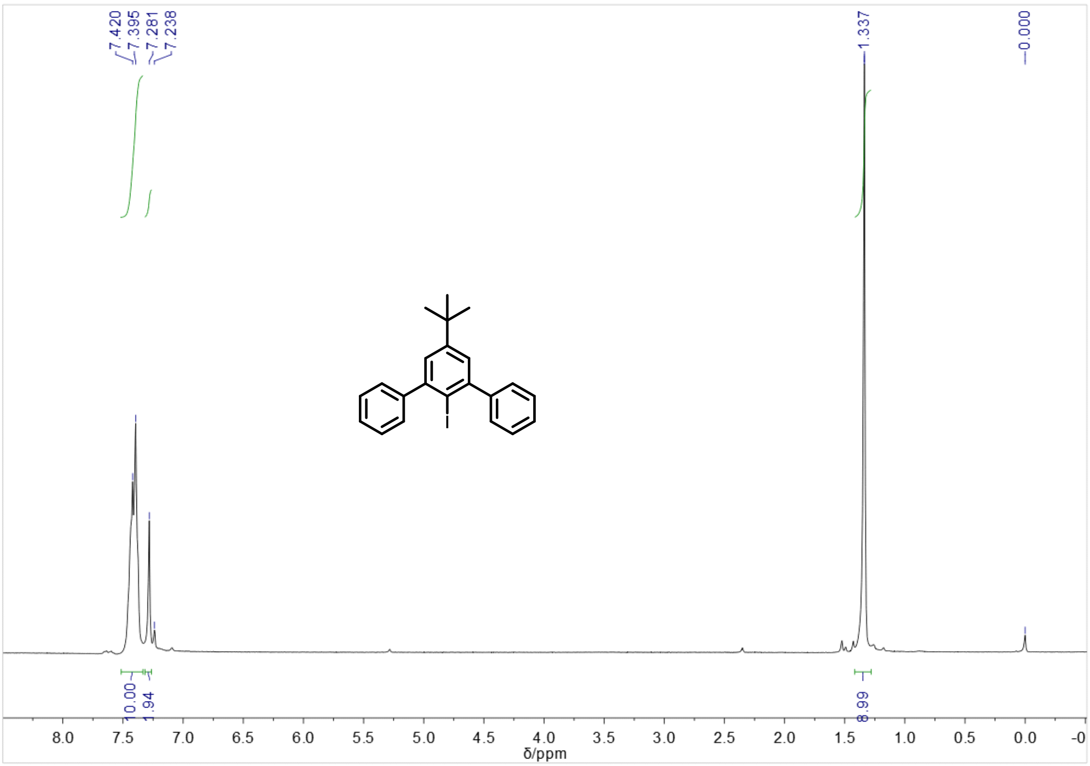

^{13}C NMR spectrum of **5** (125 M Hz, $CDCl_3$)

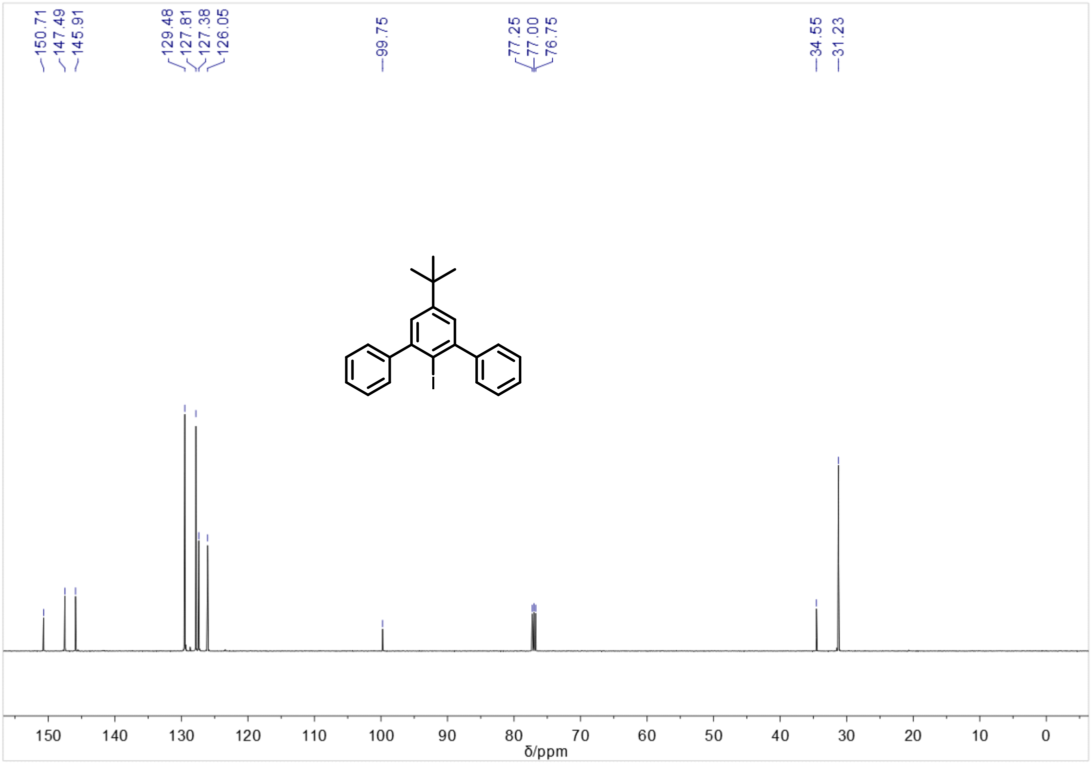

MALDI-FTICR spectra of **5**

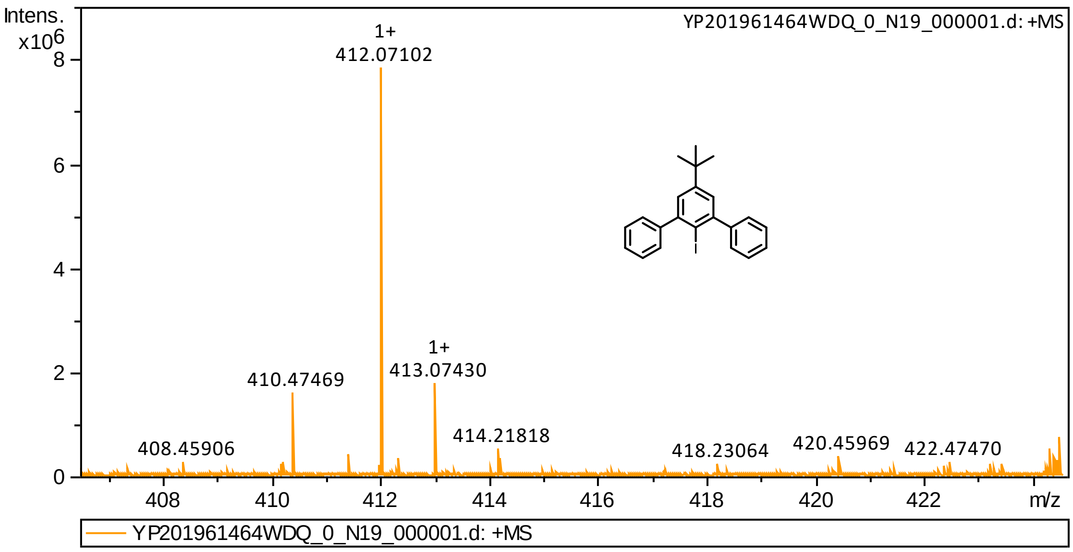

^{1}H NMR spectrum of **7** (500 M Hz, $CDCl_3$)

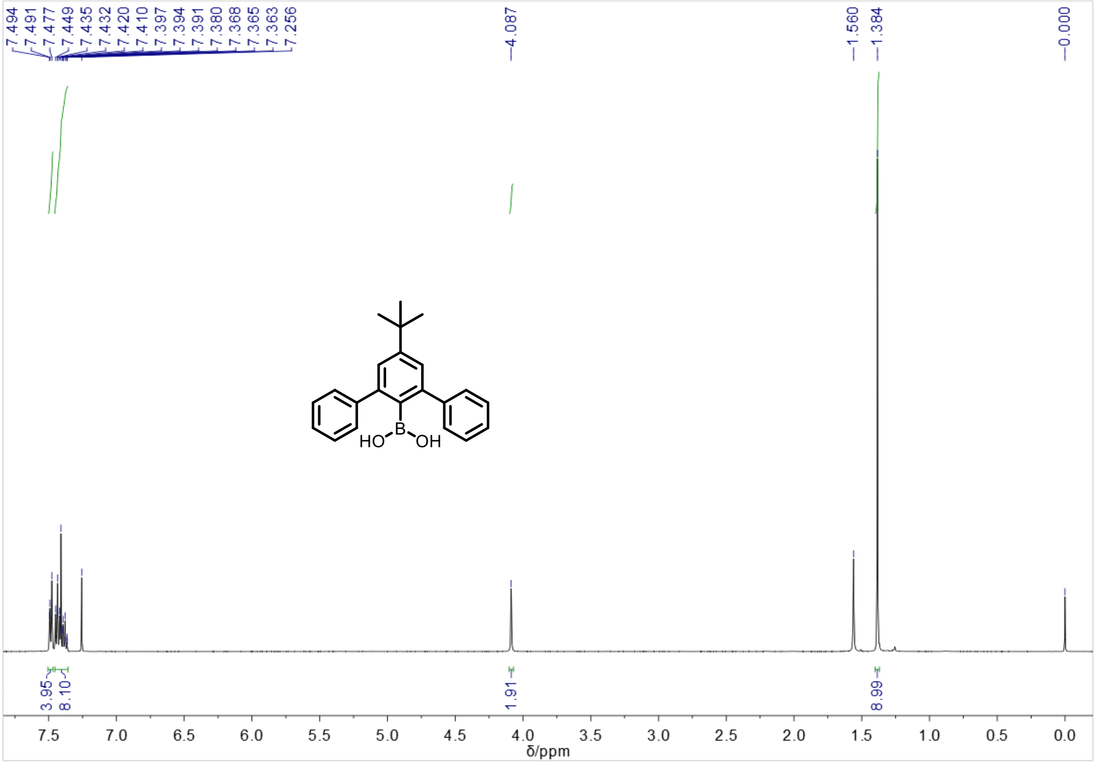

^{13}C NMR spectrum of **7** (125 M Hz, $CDCl_3$)

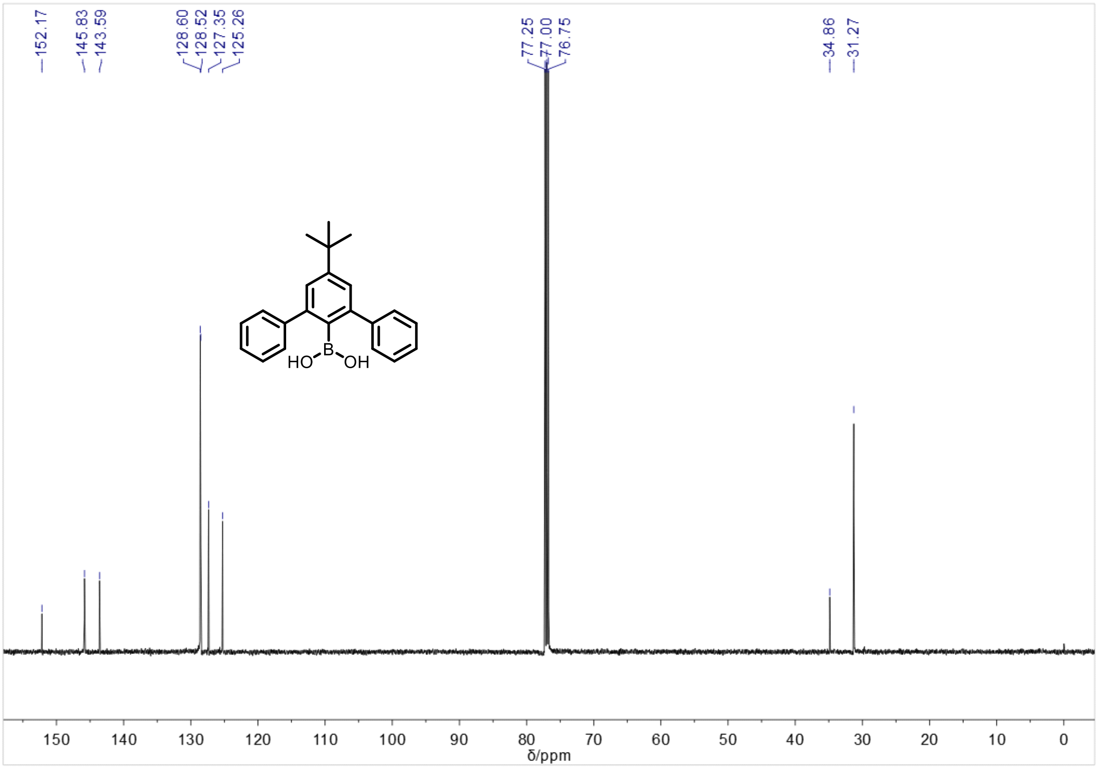

HRMS (ESI-MS) spectra of **7**

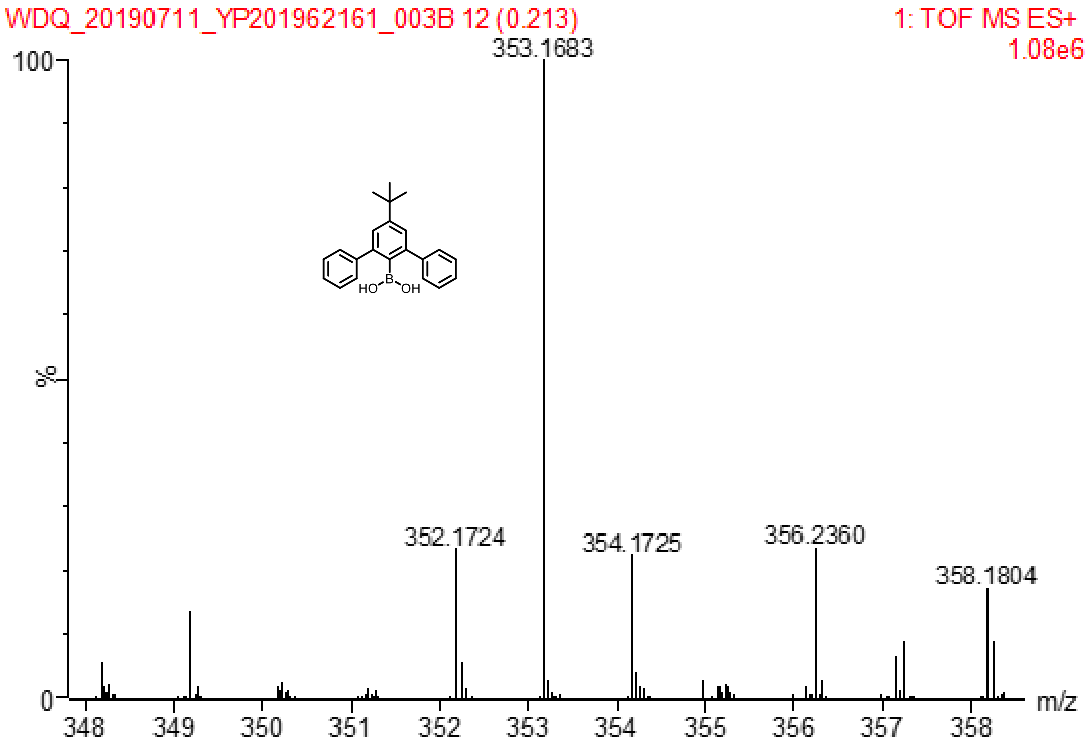

^{1}H NMR spectrum of **4** (400 M Hz, $CDCl_3$)

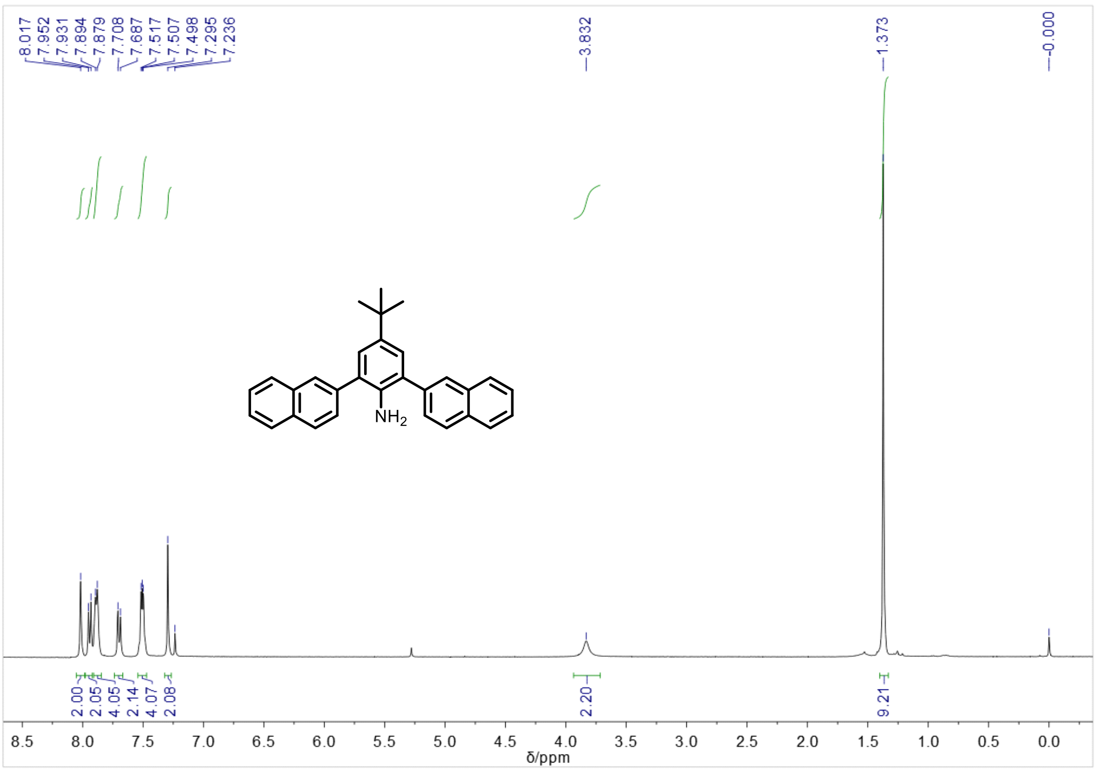

^{13}C NMR spectrum of **4** (125 M Hz, $CDCl_3$)

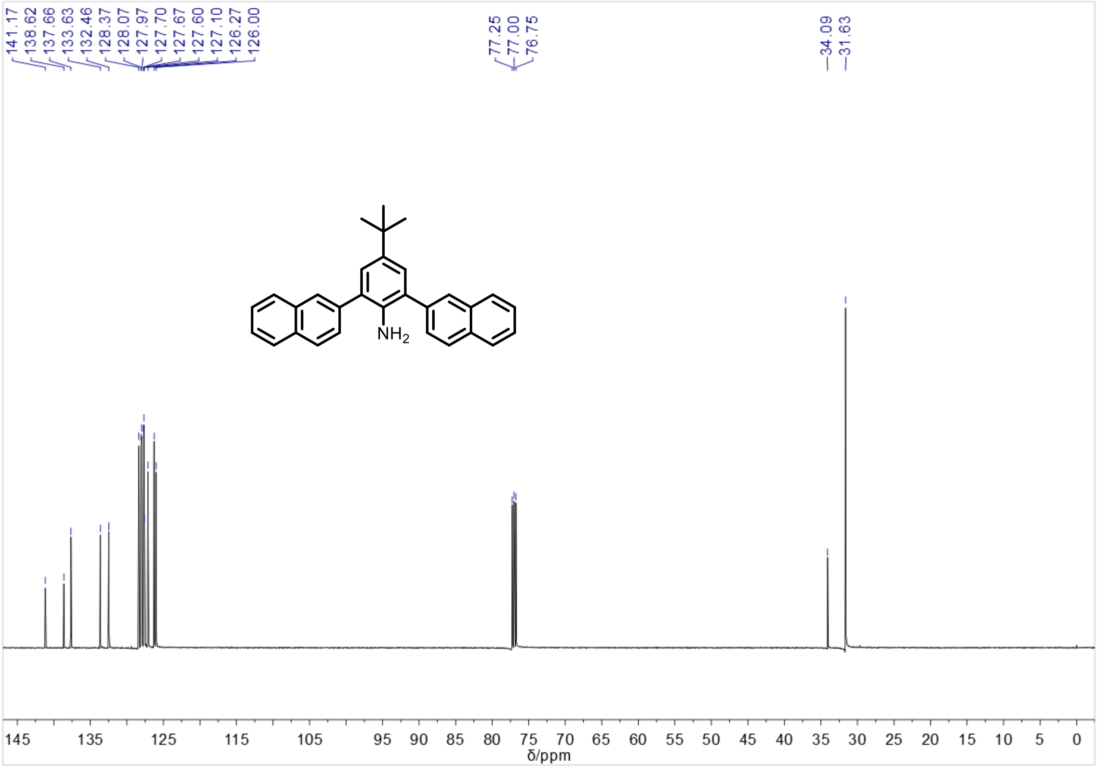

MALDI-FTICR spectra of **4**

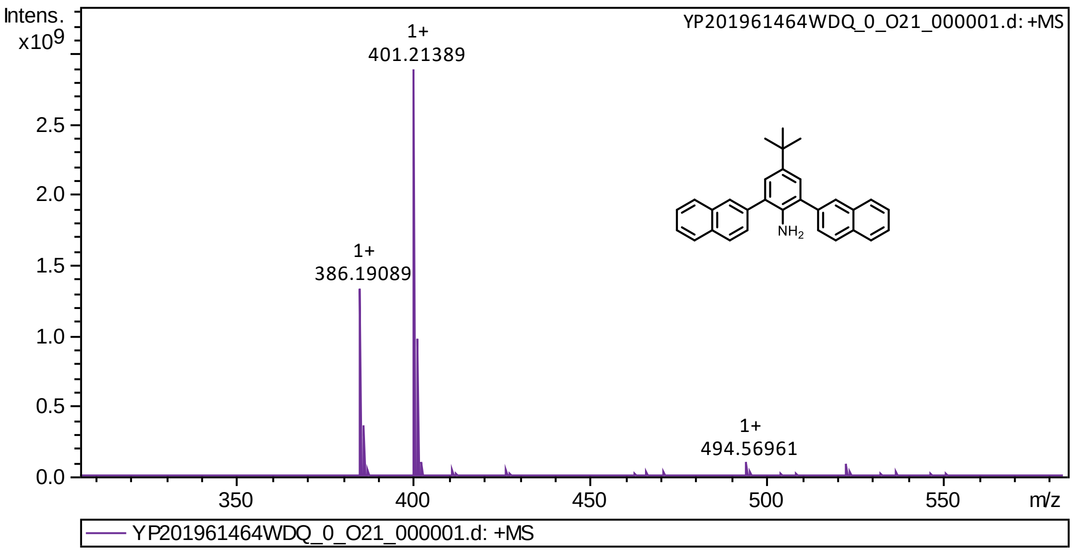

[1]H NMR spectrum of **6** (500 M Hz, $CDCl_3$)

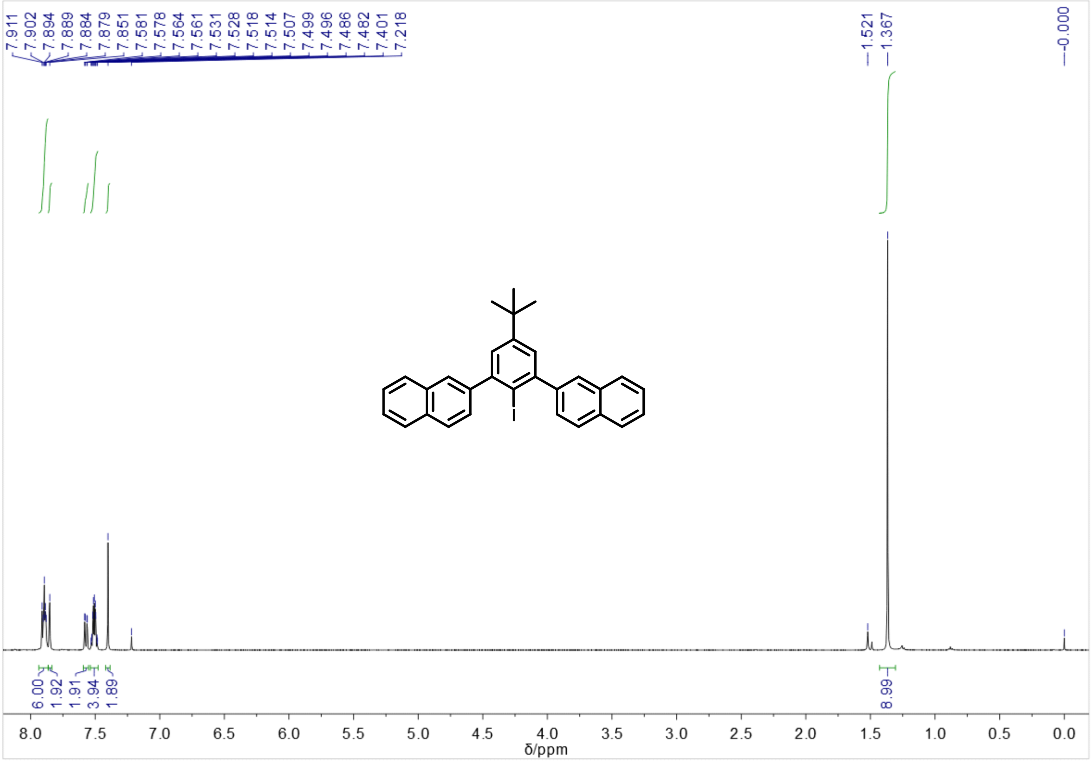

[13]C NMR spectrum of **6** (125 M Hz, $CDCl_3$)

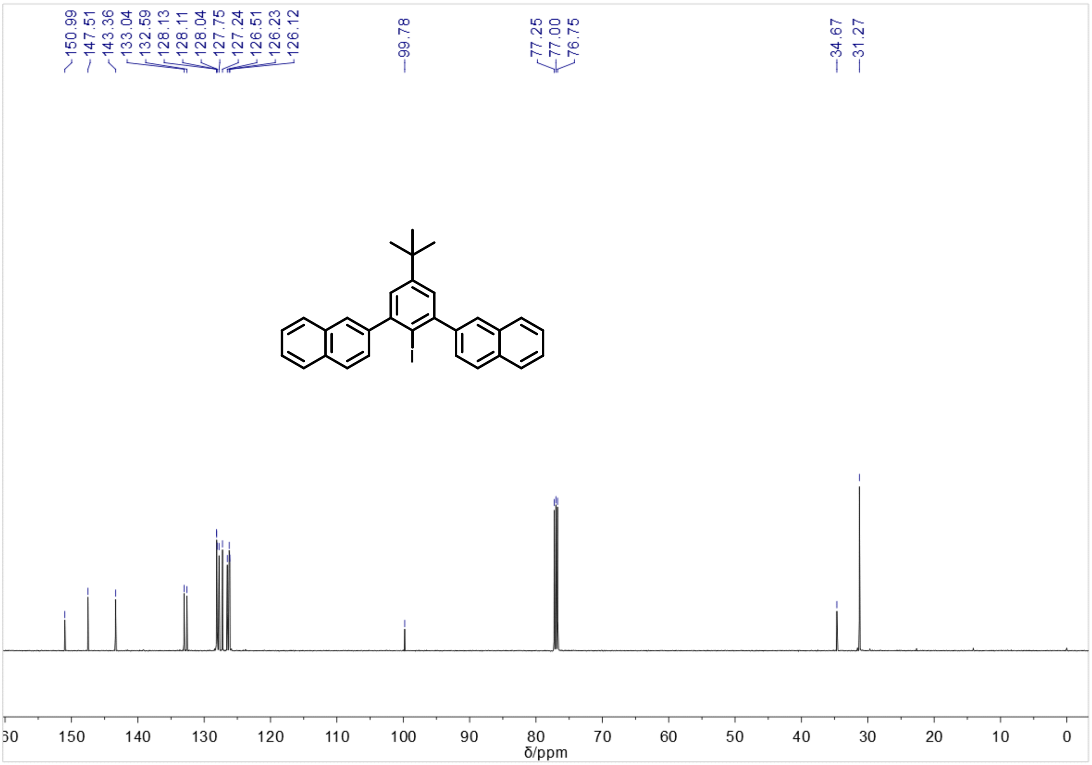

MALDI-FTICR spectra of **6**

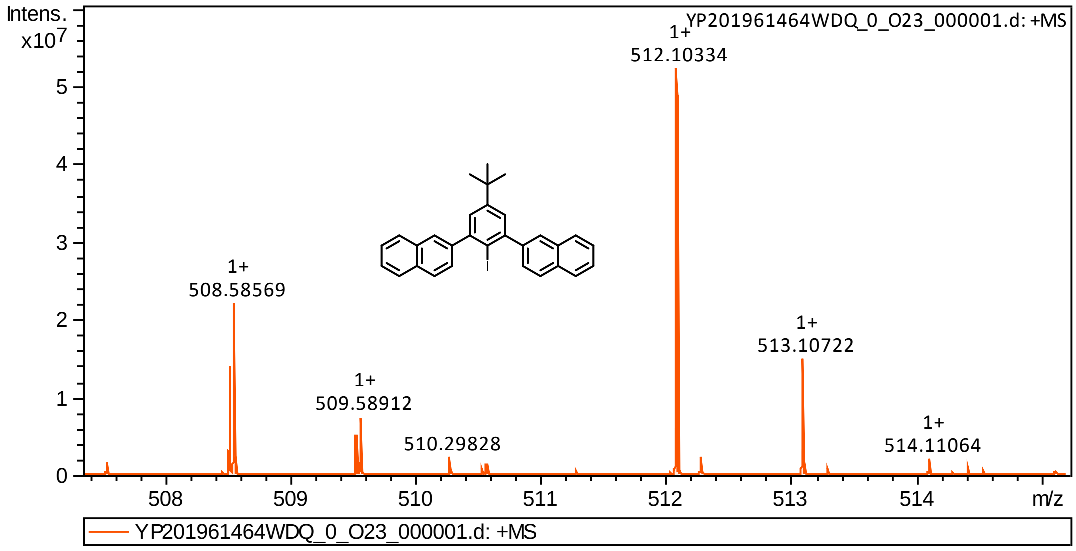

^{1}H NMR spectrum of **8** (500 M Hz, $CDCl_3$)

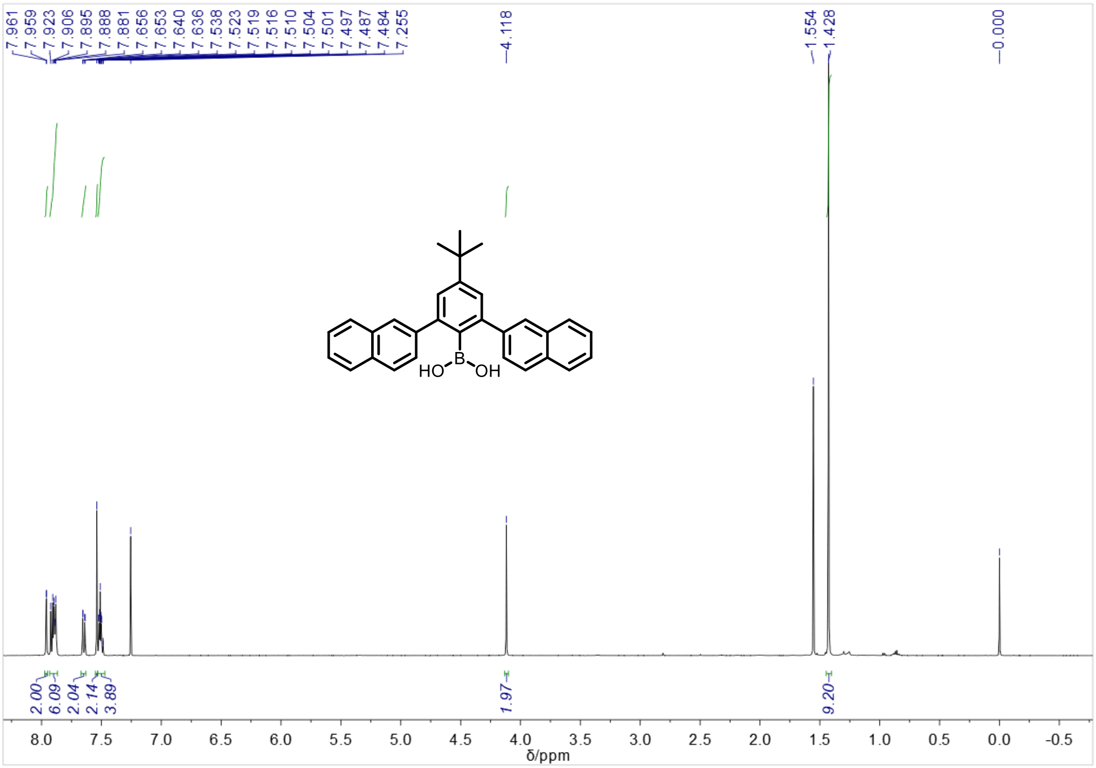

^{13}C NMR spectrum of **8**(125 M Hz, $CDCl_3$)

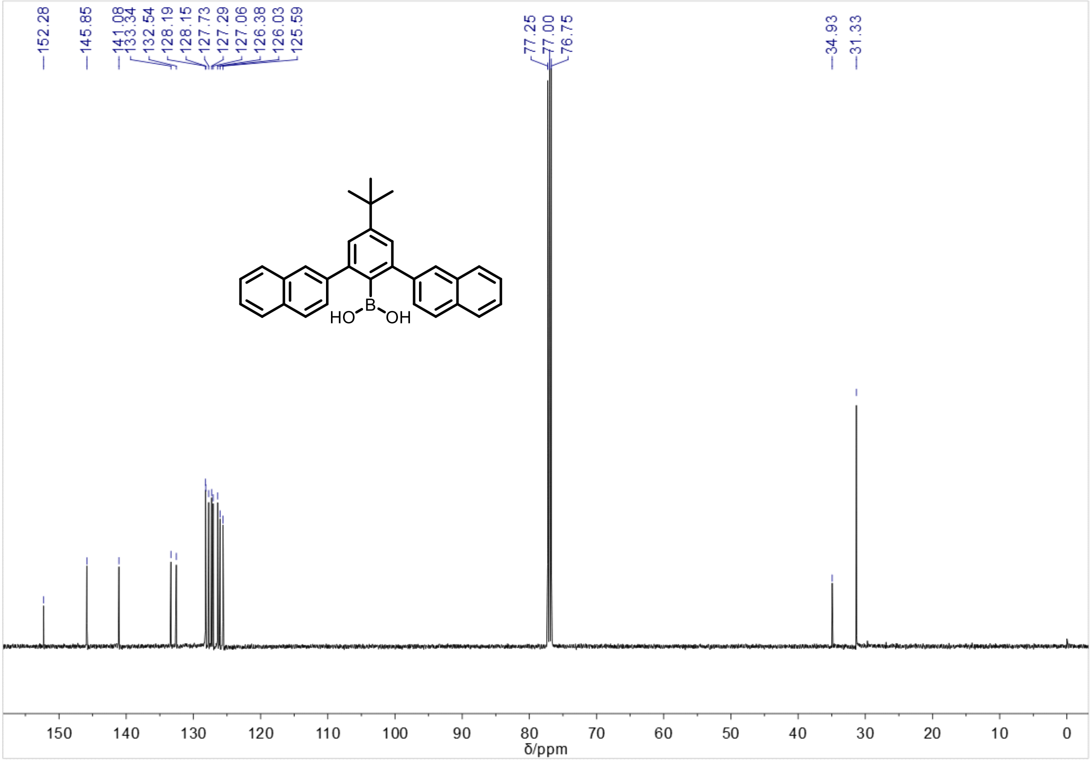

HRMS (ESI-MS) spectra of **8**

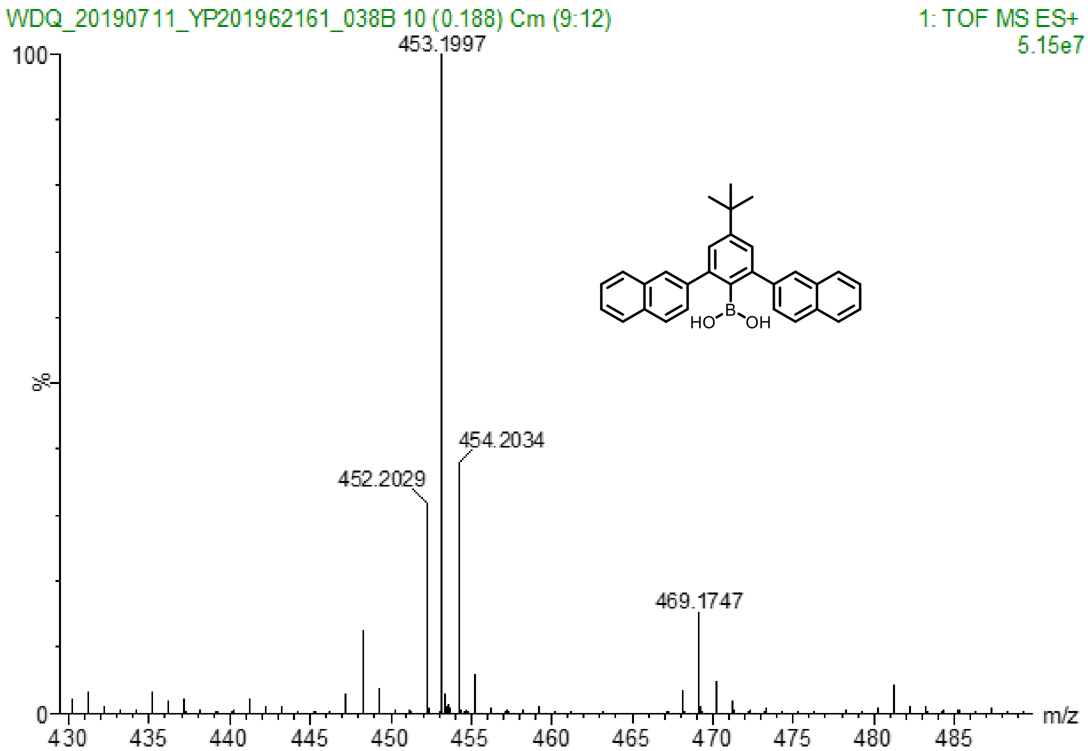

[1]H NMR spectrum of **Ph-NBN** (500 M Hz, $CDCl_3$)

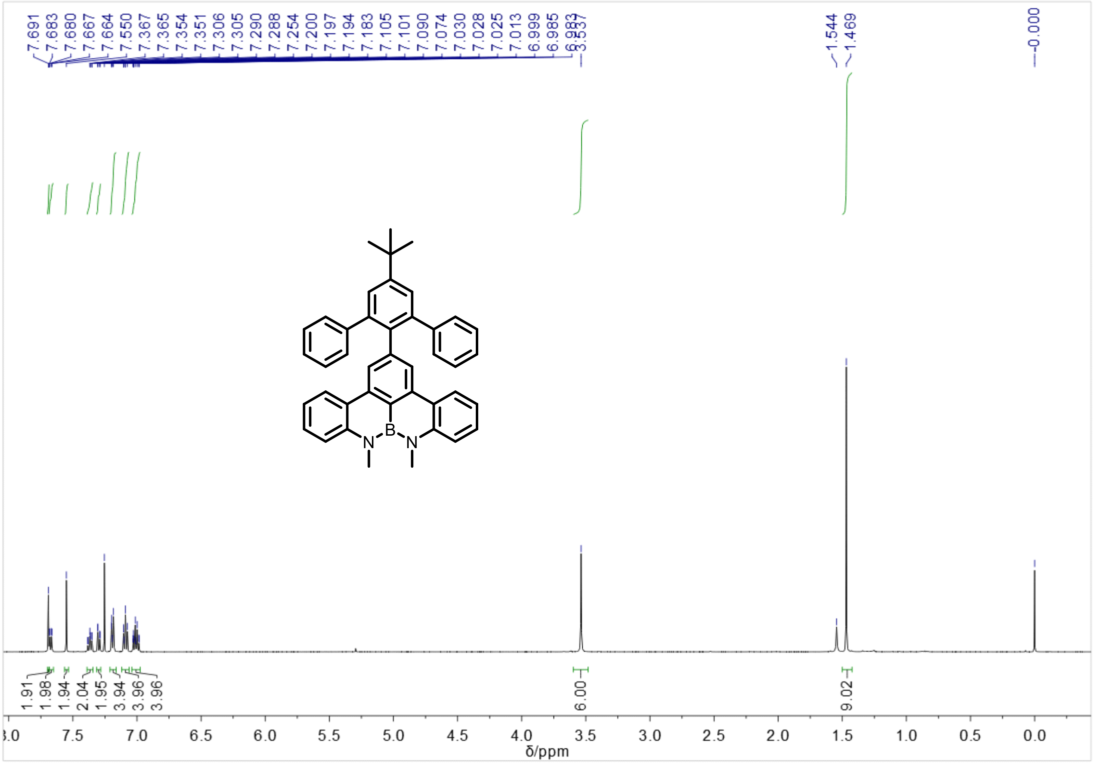

[13]C NMR spectrum of **Ph-NBN**(125 M Hz, $CDCl_3$)

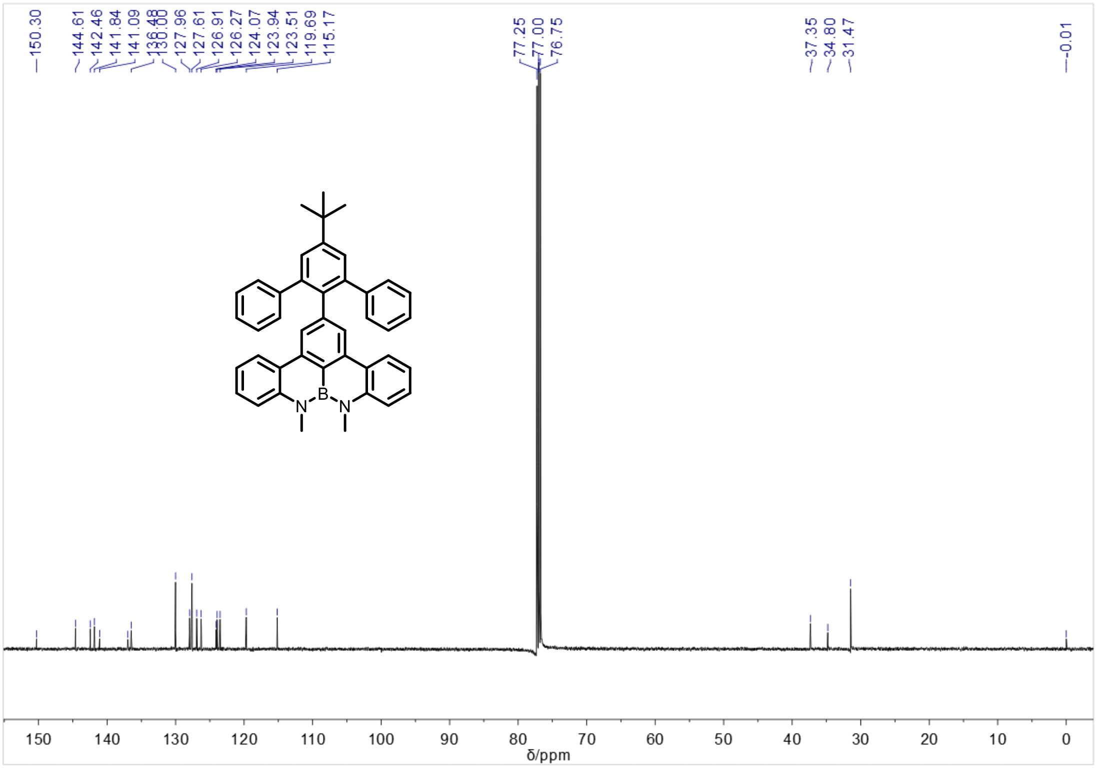

^{11}B NMR spectrum of **Ph-NBN** (225 MHz, $CDCl_3$)

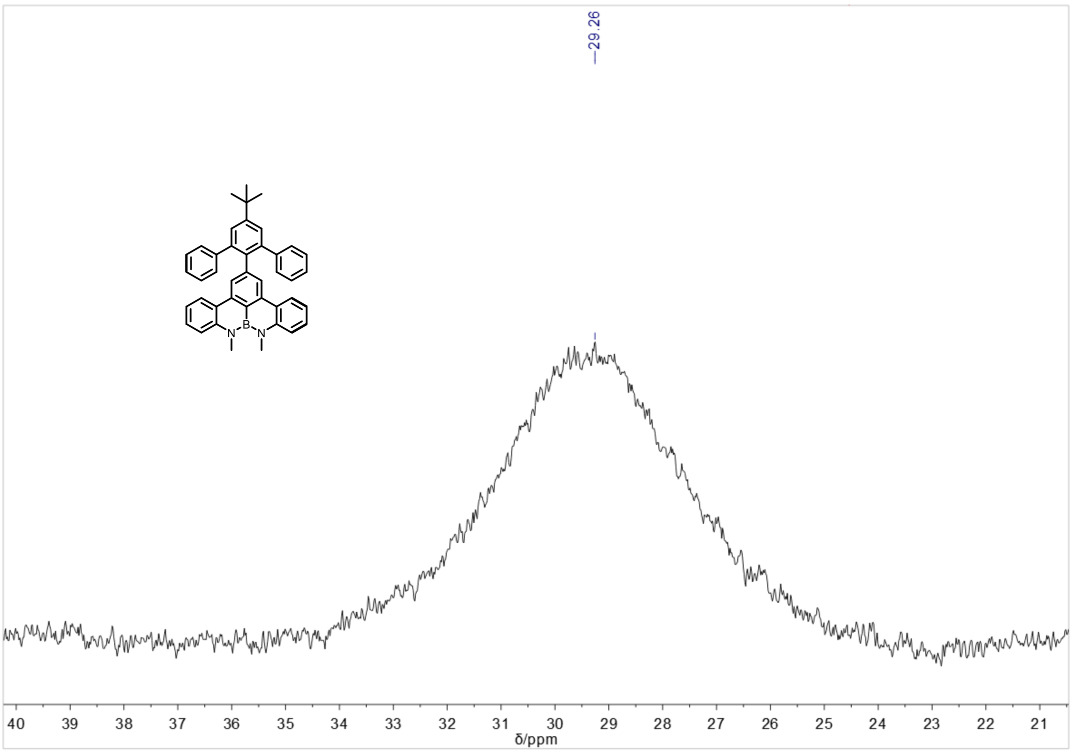

MALDI-FTICR spectra of **Ph-NBN**

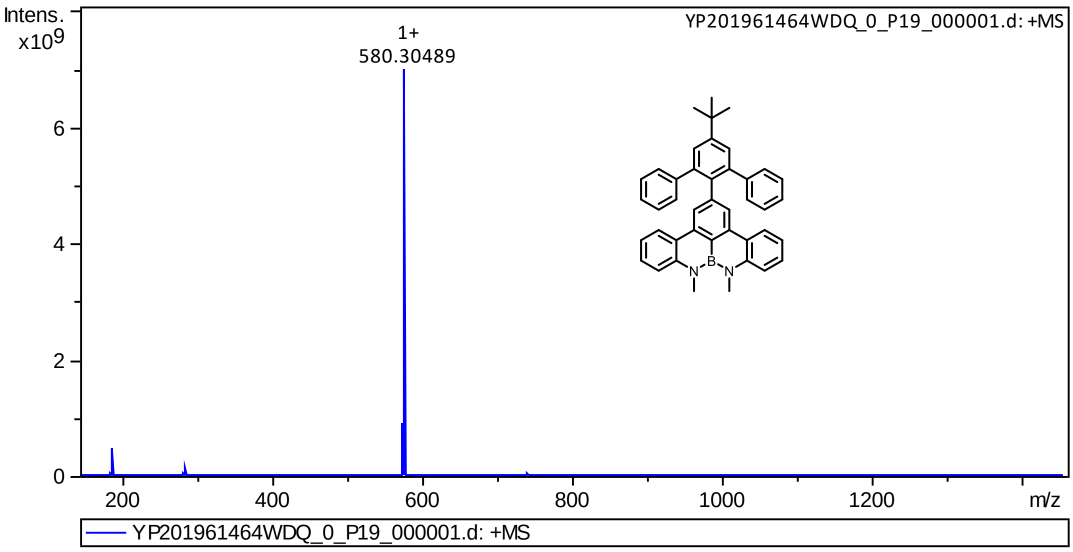

^{1}H NMR spectrum of **Ph-NBNDH** (500 M Hz, $CDCl_3$)

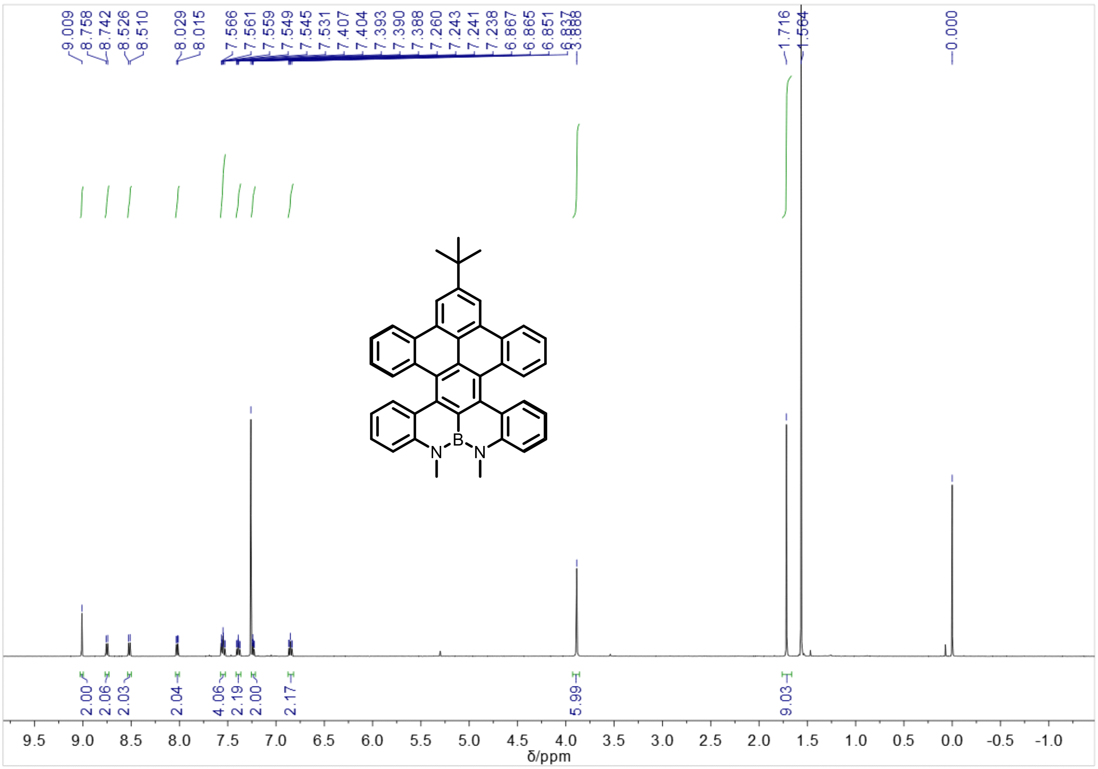

^{13}C NMR spectrum of **Ph-NBNDH**(125 M Hz, $CDCl_3$)

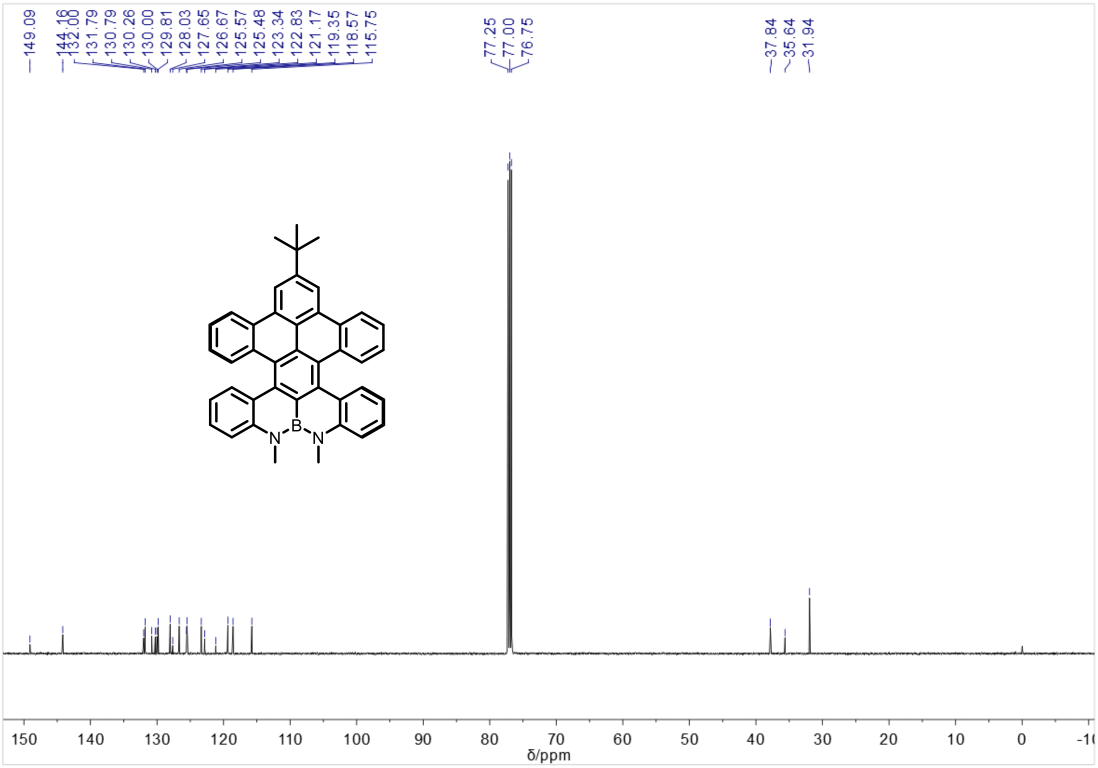

^{11}B NMR spectrum of **Ph-NBNDH** (225 MHz, $CDCl_3$)

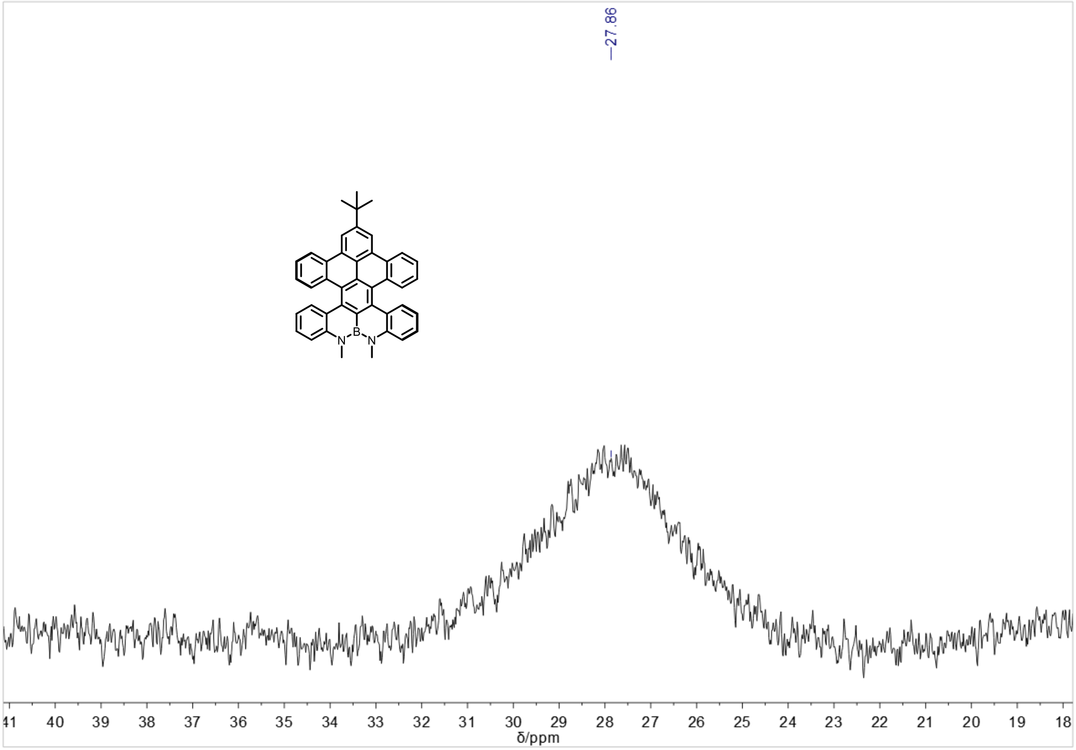

MALDI-FTICR spectra of **Ph-NBNDH**

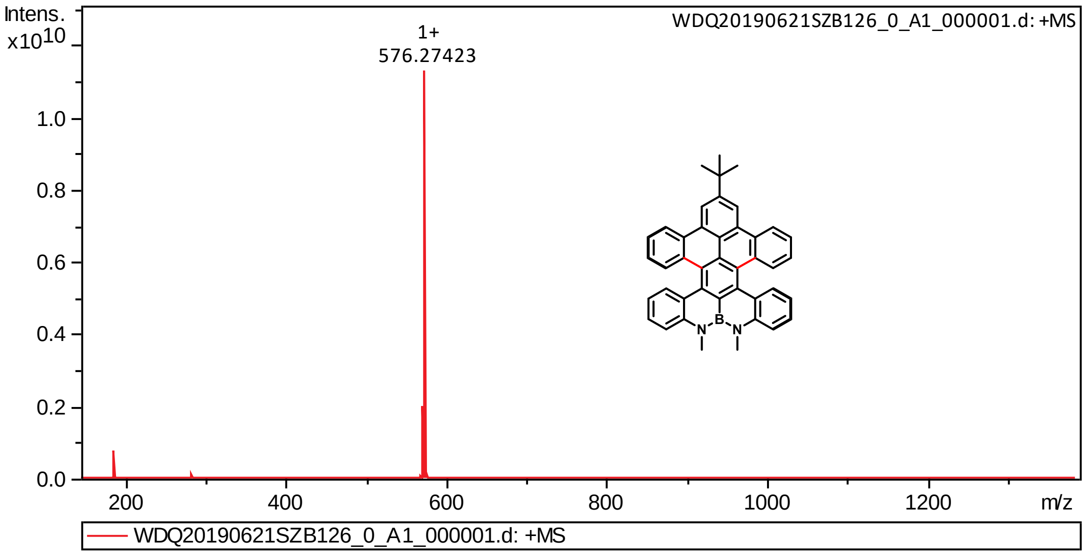

^{1}H NMR spectrum of **Naph-NBN** (400 M Hz, $CDCl_3$)

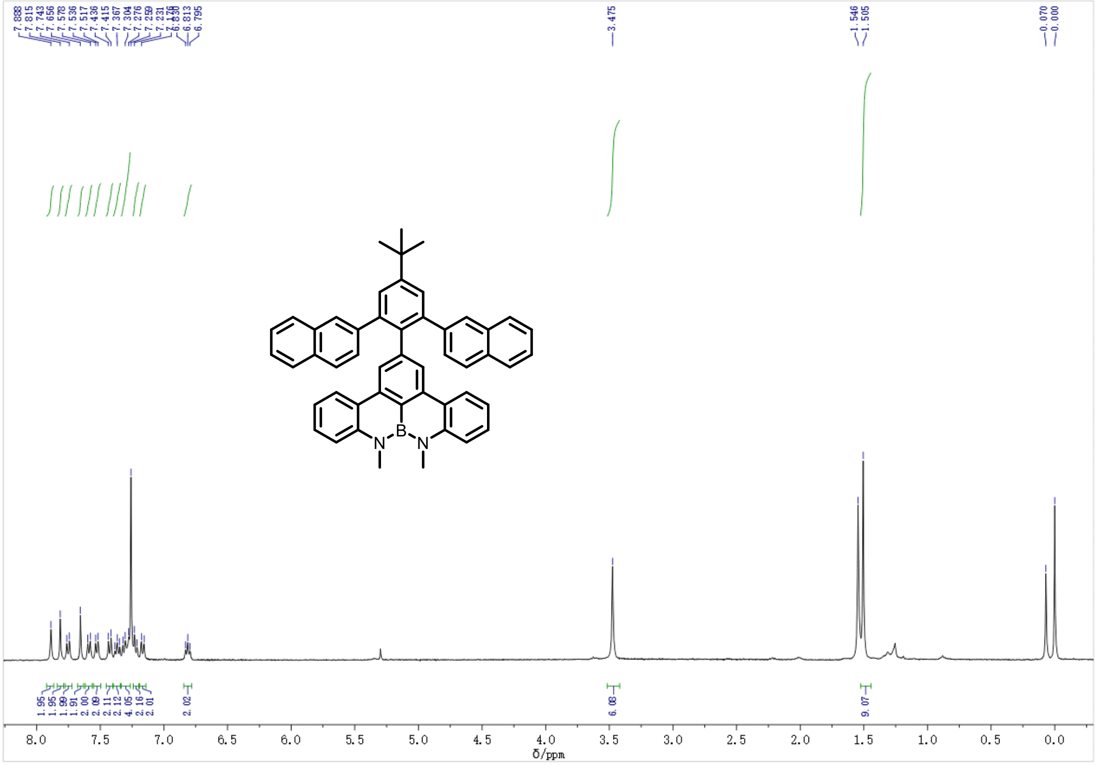

^{13}C NMR spectrum of **Naph-NBN**(125 M Hz, $CDCl_3$)

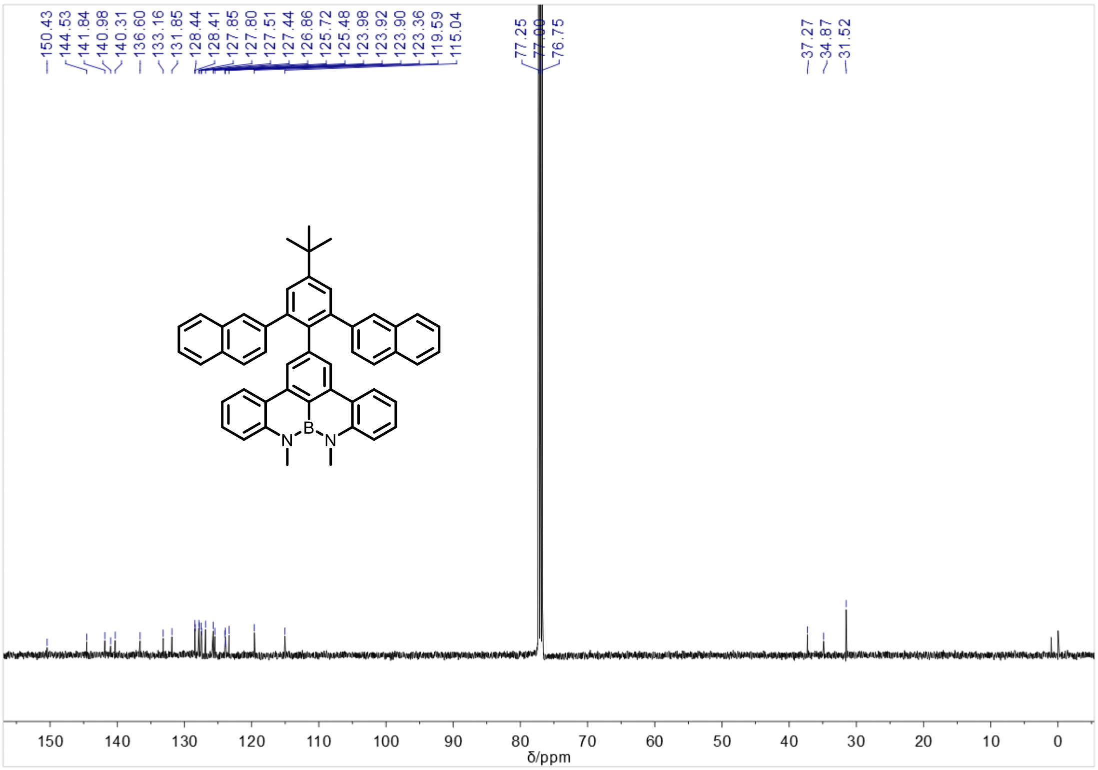

^{11}B NMR spectrum of **Naph-NBN** (225 MHz, $CDCl_3$)

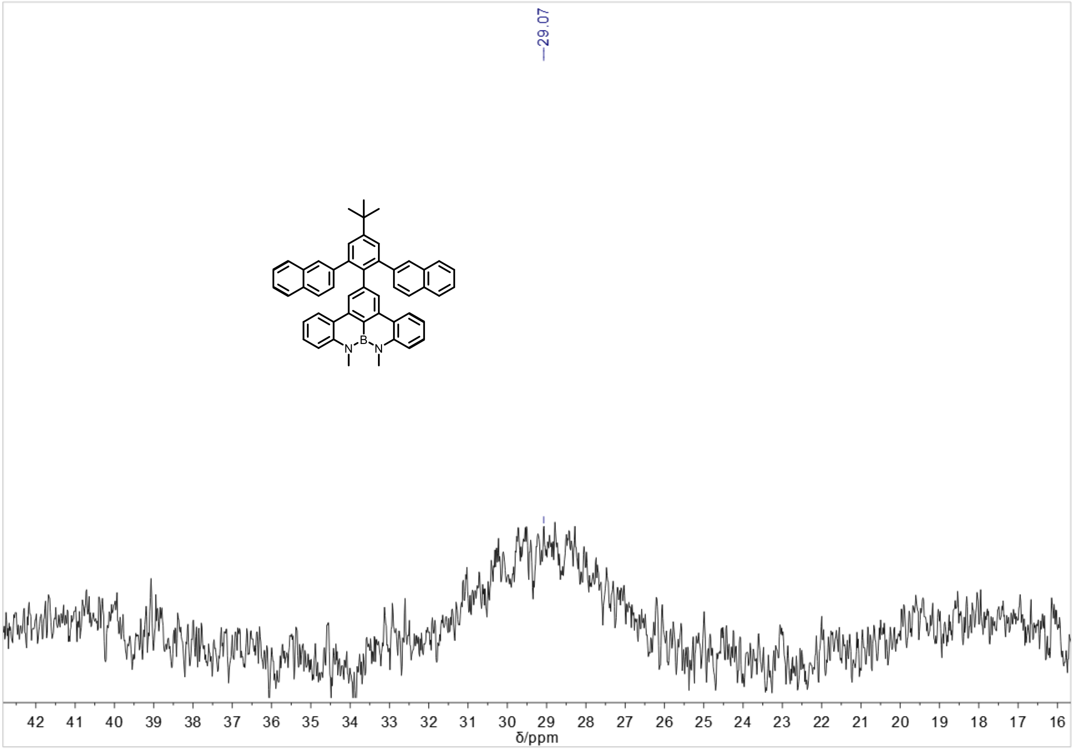

MALDI-FTICR spectra of **Naph-NBN**

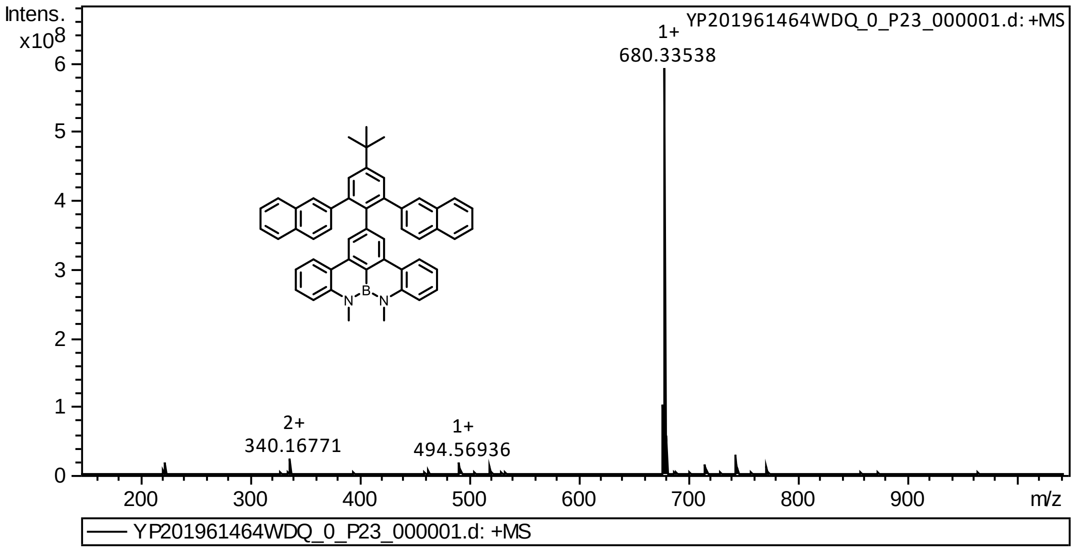

[1]H NMR spectrum of **Naph-NBNDH** (400 M Hz, $CDCl_3$)

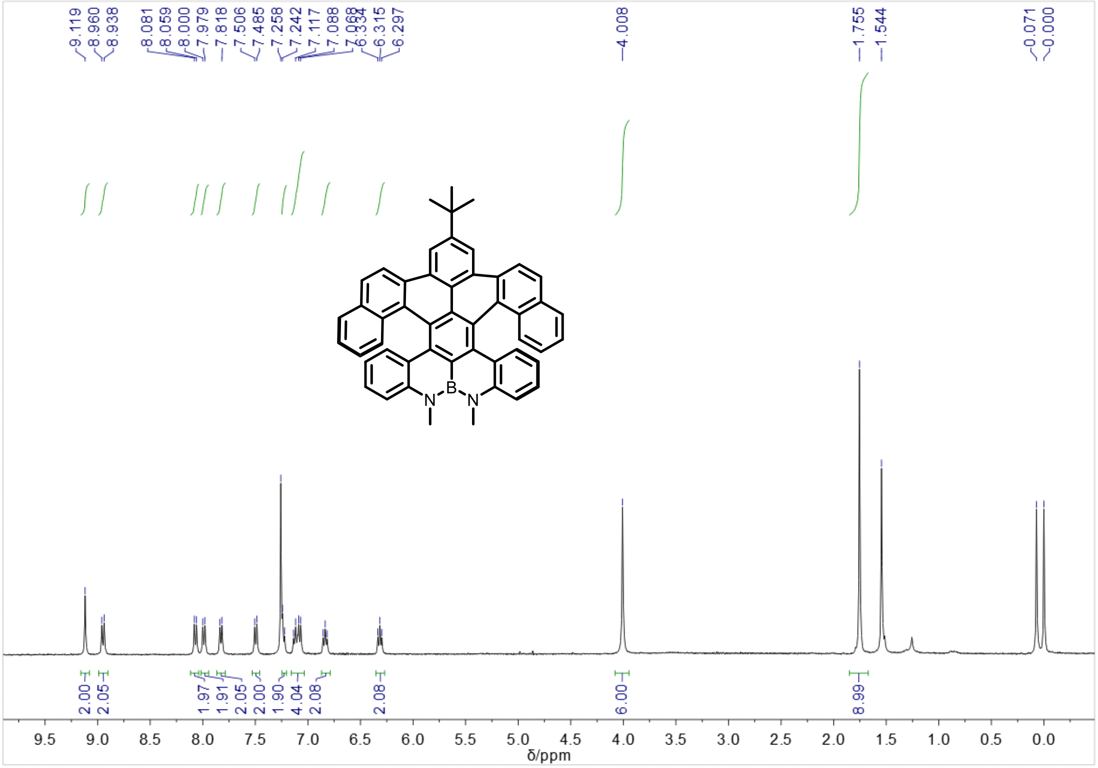

[13]C NMR spectrum of **Naph-NBNDH**(125 M Hz, $CDCl_3$)

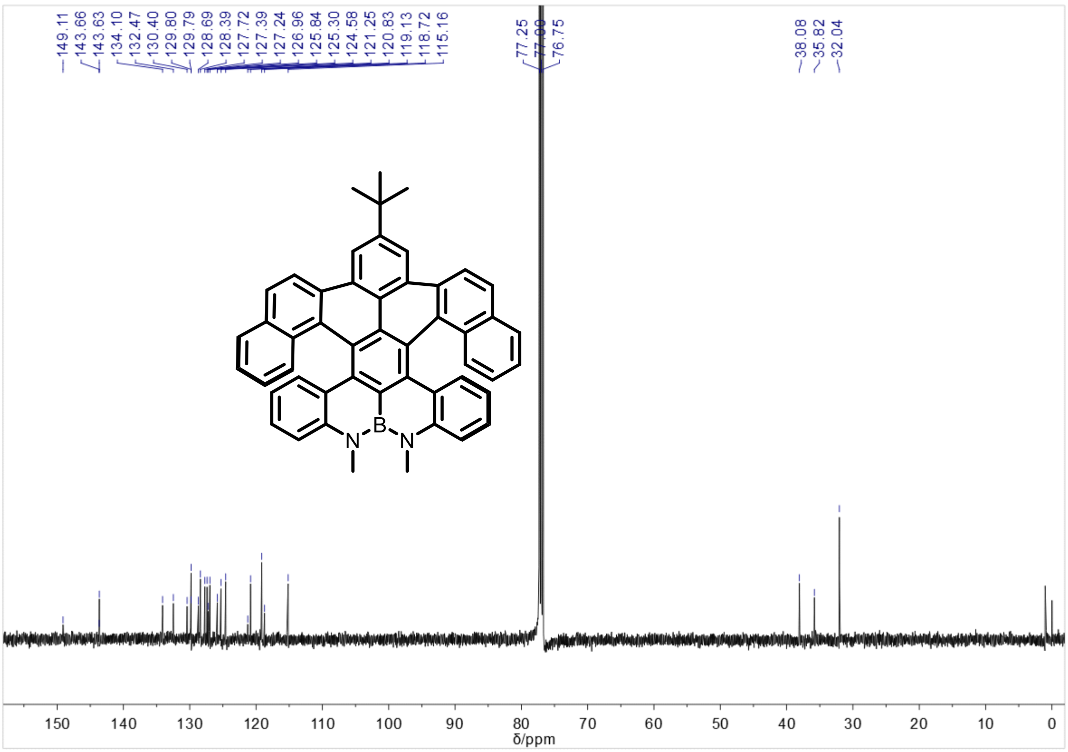

^{11}B NMR spectrum of **Naph-NBNDH** (225 MHz, $CDCl_3$)

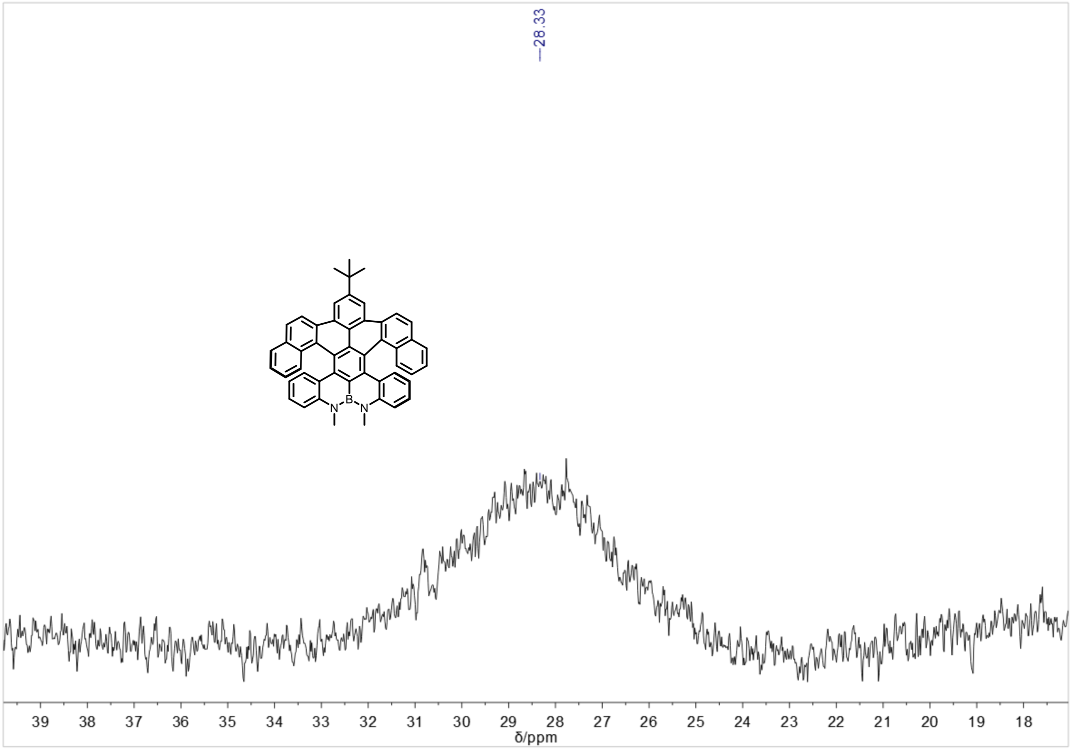

MALDI-FTICR spectra of **Naph-NBNDH**

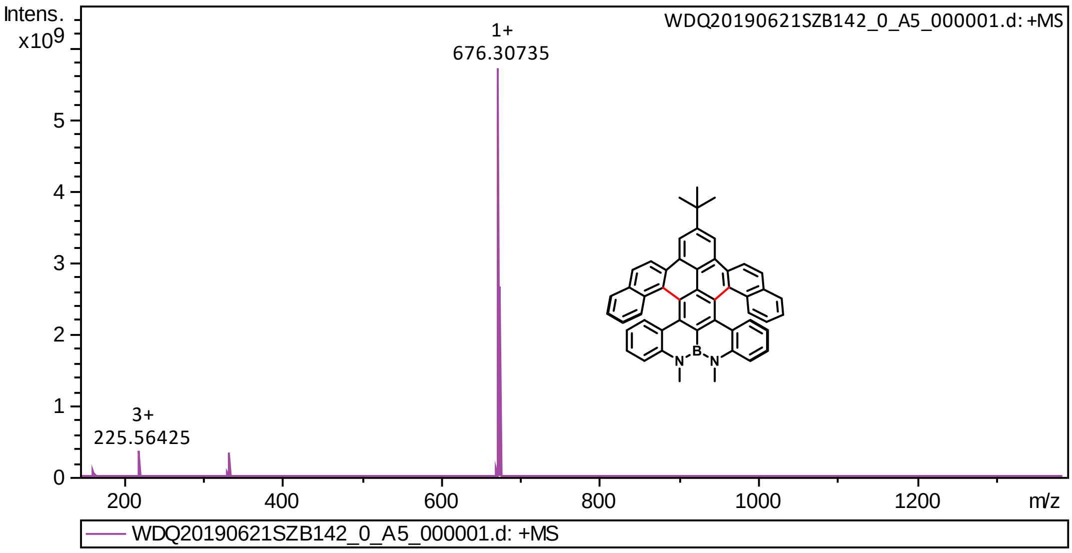

Reference:

S1. Schlütter, F.; Nishiuchi, T.; Enkelmann, V.; Müllen, K. *Polymer Chemistry* **2013**, *4*, 2963.

S2. SHELXL-97, Program for the Refinement of Crystal Structure, Sheldrick, G. M. University of Götingen, Götingen (Germany), **1997**.

S3. Gaussian 09, Revision D.01, M. J. Frisch, G. W. Trucks, H. B. Schlegel, G. E. Scuseria, M. A. Robb, J. R. Cheeseman, G. Scalmani, V. Barone, B. Mennucci, G. A. Petersson, H. Nakatsuji, M. Caricato, X. Li, H. P. Hratchian, A. F. Izmaylov, J. Bloino, G. Zheng, J. L. Sonnenberg, M. Hada, M. Ehara, K. Toyota, R. Fukuda, J. Hasegawa, M. Ishida, T. Nakajima, Y. Honda, O. Kitao, H. Nakai, T. Vreven, J. A. Montgomery, Jr., J. E. Peralta, F. Ogliaro, M. Bearpark, J. J. Heyd, E. Brothers, K. N. Kudin, V. N. Staroverov, R. Kobayashi, J. Normand, K. Raghavachari, A. Rendell, J. C. Burant, S. S. Iyengar, J. Tomasi, M. Cossi, N. Rega, J. M. Millam, M. Klene, J. E. Knox, J. B. Cross, V. Bakken, C. Adamo, J. Jaramillo, R. Gomperts, R. E. Stratmann, O. Yazyev, A. J. Austin, R. Cammi, C. Pomelli, J. W. Ochterski, R. L. Martin, K. Morokuma, V. G. Zakrzewski, G. A. Voth, P. Salvador, J. J. Dannenberg, S. Dapprich, A. D. Daniels, Ö. Farkas, J. B. Foresman, J. V. Ortiz, J. Cioslowski, and D. J. Fox, Gaussian, Inc., Wallingford CT, **2009**.

S4. (a) Fujikawa, T.; Segawa, Y.; Itami, K. *J. Am. Chem. Soc.* **2015**, *137*, 7763. (b) Hosokawa, T.; Takahashi, Y.; Matsushima, T.; Watanabe, S.; Kikkawa, S.; Azumaya, I.; Tsurusaki, A.; Kamikawa, K. *J. Am. Chem. Soc.* **2017**, *139*, 18512. (c) Hu, Y.; Wang, X. Y.; Peng, P. X.; Wang, X. C.; Cao, X. Y.; Feng, X.; Müllen, K.; Narita, A. *Angew. Chem. Int. Ed.* **2017**, *56*, 3374. (d) Hu, Y.; Paterno, G. M.; Wang, X. Y.; Wang, X. C.; Guizzardi, M.; Chen, Q.; Schollmeyer, D.; Cao, X. Y.; Cerullo, G.; Scotognella, F.; Müllen, K.; Narita, A. *J. Am. Chem. Soc.* **2019**, *141*, 12797. (e) Kato, K.; Segawa, Y.; Scott, L. T.; Itami, K. *Angew. Chem. Int. Ed.* **2018**, *57*, 1337. (f) Tanaka, H.; Ikenosako, M.; Kato, Y.; Fujiki, M.; Inoue, Y.; Mori, T. *Commun. Chem.* **2018**, *1*,38. (g) Wang, Y.; Yin, Z.; Zhu, Y.; Gu, J.; Li, Y.; Wang, J. *Angew. Chem. Int. Ed.* **2019**, *58*, 587. (h) Yamano, R.; Shibata, Y.; Tanaka, K. *Chem.* **-** *Eur. J.* **2018**, *24*, 6364. (i) Zhu, Y.; Guo, X.; Li, Y.; Wang, J. *J. Am. Chem. Soc.* **2019**, *141*, 5511.

S5. (a) Fujikawa, T.; Mitoma, N.; Wakamiya, A.; Saeki, A.; Segawa, Y.; Itami, K. *Org. Biomol. Chem.* **2017**, *15*, 4697. (b) Fujikawa, T.; Segawa, Y.; Itami, K. *J. Am. Chem. Soc.* **2016**, *138*, 3587. (c) Katayama, T.; Nakatsuka, S.; Hirai, H.; Yasuda, N.; Kumar, J.; Kawai, T.; Hatakeyama, T. *J. Am. Chem. Soc.* **2016**, *138*, 5210. (d) Wang, X. Y.; Narita, A.; Zhang, W.; Feng, X.; Müllen, K. J. Am. Chem. Soc. 2016, 138, 9021. (e) Wang, X. Y.; Dienel, T.; Di Giovannantonio, M.; Barin, G. B.; Kharche, N.; Deniz, O.; Urgel, J. I.; Widmer, R.; Stolz, S.; De Lima, L. H.; Muntwiler, M.; Tommasini, M.; Meunier, V.; Ruffieux, P.; Feng, X.; Fasel, R.; Müllen, K.; Narita, A. *J. Am. Chem. Soc.* **2017**, *139*, 4671. (f) Wang, X. Y.; Wang, X. C.; Narita, A.; Wagner, M.; Cao, X. Y.; Feng, X.; Müllen, K. *J. Am. Chem. Soc.* **2016**, *138*, 12783. (g) Lin, H. A.; Kato, K.; Segawa, Y.; Scott, L. T.; Itami, K. *Chem. Sci.* **2019**, *10*, 2326. (h) Liu, G.; Koch, T.; Li, Y.; Doltsinis, N. L.; Wang, Z. *Angew. Chem. Int. Ed.* **2019**, *58*, 178. (i) Meng, D.; Liu, G.; Xiao, C.; Shi, Y.; Zhang, L.; Jiang, L.; Baldridge, K. K.; Li, Y.; Siegel, J. S.; Wang, Z. *J. Am. Chem. Soc.* **2019**, *141*, 5402. (j) Nakamura, K.; Furumi, S.; Takeuchi, M.; Shibuya, T.; Tanaka, K. *J. Am. Chem. Soc.* **2014**, *136*, 5555. (k) Sakamaki, D.; Kumano, D.; Yashima, E.; Seki, S. *Angew. Chem. Int. Ed.* **2015**, *54*, 5404. (l) Schuster, N. J.; Hernandez Sanchez, R.; Bukharina, D.; Kotov, N. A.; Berova, N.; Ng, F.; Steigerwald, M. L.; Nuckolls, C.

J. Am. Chem. Soc. **2018**, *140*, 6235. (m) Zeng, C.; Xiao, C.; Feng, X.; Zhang, L.; Jiang, W.; Wang, Z. *Angew. Chem. Int. Ed.* **2018**, *57*, 10933.